Received: 5 January 2022 | Revised: 13 April 2022 | Accepted: 20 April 2022

DOI: 10.1111/bre.12673

Basin Research | IAS EAGE | WILEY

RESEARCH ARTICLE

Contractional salt deformation in a recently inverted basin: Miocene to current salt deformation within the central Algerian basin

Simon Blondel[1,2] | **Massimo Bellucci**[3,4] | **Sian Evans**[5] | **Anna Del Ben**[2] | **Angelo Camerlenghi**[1]

[1]National Institute of Oceanography and Applied Geophysics OGS, Trieste, Italy

[2]Department of Mathematics and Geosciences, University of Trieste, Trieste, Italy

[3]Department of Marine Geosciences, Ifremer, Plouzané, France

[4]SAIPEM SA, Montigny-le-Bretonneux, France

[5]Department of Geosciences, University of Oslo, Oslo, Norway

Correspondence
Simon Blondel, National Institute of Oceanography and Applied Geophysics OGS, Trieste, Italy.
Email: simon.blondel2@gmail.com

Funding information
This research is carried out under the SALTGIANT ETN, a European project funded by the European Union's Horizon 2020 research and innovation programme under the Marie Skłodowska-Curie grant agreement n° 765256. The SALTFLU seismic profiles of the Algero-Balearic margin were acquired within EUROFLEETS, call for ship-time 'Ocean' 2010, project 'Salt deformation and sub-salt fluid circulation in the Algero-Balearic abyssal plain—SALTFLU'

Abstract

Field analogues illustrating the early stage of deformation of shortening structures in salt-bearing orogenic fold-and-thrust belts are not yet well illustrated in literature. The relatively young Messinian salt of the Algerian basin could represent a good case example of such systems. The Algerian Basin is a deep-water Miocene back-arc basin including a layer of mobile Messinian evaporites up to 2 km thick. The Messinian salt was deposited in an already inverted basin, after its extensive stage. Its inversion initiated in the Tortonian, with a N-NW shortening induced by the north-westward motion of the African plate. In this study, we use new 2D multichannel seismic data to identify, classify and map salt structures throughout the central Algerian Basin and re-assess its structural style. We interpret contractional salt tectonic structures, such as buckle folds, squeezed diapirs and related salt sheets as evidence of regional thick-skinned shortening episodes. We conclude that horizontal displacement loading has driven salt deformation within the basin since its deposition. We also show spatial variations in the structural style of the central Algerian Basin, both along- and down-dip. We demonstrate that the initial shortening-related salt deformation in the late Messinian was focussed along the Algerian margin and later shifted outward toward the Balearic margin in the Plio-Quaternary. The shifting of the deformation front is interpreted to be a result of the thickening and strengthening of the overburden. The second peak of deformation may have reactivated faults along the Emile-Baudot escarpment with thick-skinned deformation. We also observe a variation in the intensity of the salt deformation along the margin from SW to NE, which may be due to variable tectonic loading applied along the Algerian margin or the pre-shortening distribution of salt.

KEYWORDS

active margins, Algerian basin, Algero-Balearic basin, contractional salt system, Messinian Salinity Crisis, salt tectonics

1 | INTRODUCTION

Contractional salt tectonic systems encompass settings where widespread shortening is applied to a salt layer (Jackson & Hudec, 2017). They are commonly described within three distinct geological settings (Jackson & Hudec, 2017; Letouzey et al., 1995): (i) gravity-driven deformation on a continental margin; (ii) thick-skinned inversion of an extended intracratonic basin and (iii) orogenic shortening on a convergent or collisional margin driven by subduction. While gravity-driven, salt-detached deep-water fold belts are well-documented (e.g. Davison et al., 2012; Jackson et al., 2015; Lundin, 1992; Quirk et al., 2012; Rowan et al., 2004), thick-skinned contractional salt systems are not as well imaged and relatively less-understood.

Thick-skinned, orogenic fold belts display similar salt structures to thin-skinned, gravity-driven fold belts, such as salt-cored anticlines, box folds, squeezed diapirs, salt-detached thrusts and extruded salt sheets, with tens of kilometres of lateral displacement driven by horizontal tectonic loading (Davis & Engelder, 1985; Granado et al., 2018). This style of deformation is due to the mechanical weakness of salt compared to most lithologies (Jackson & Vendeville, 1994; Weijermars et al., 1993), thus its presence yields a large influence on the structural development of fold-and-thrust belts (Duffy et al., 2018). The weak salt layer acts as a decollement surface, decoupling the thin- and thick-skinned deformation and allowing the horizontal strain to propagate far out into the basin with a low-angle taper (Davis & Engelder, 1985; Letouzey et al., 1995). Parameters influencing the localisation of deformation include: the relative thicknesses of overburden and salt, the strain magnitude, the base-salt relief, and the presence and distribution of pre-existing structures prior to the onset of shortening (Dooley et al., 2009; Duffy et al., 2018; Jackson & Hudec, 2017; Letouzey et al., 1995; Li et al., 2021; Pichel et al., 2019; Uranga et al., 2022).

Natural examples of thick-skinned, salt-detached fold-and-thrust belts are dominantly long-lived systems, where the orogenic shortening was applied to an already deformed basin with heterogeneously distributed salt. Known field examples include: the south-western subalpine French Alps (Graham et al., 2012), the Rif-Betics (Flinch & Soto, 2017), the Atlas mountains (Vergés et al., 2017), the Pyrénées (Sans & Vergés, 1996), the Zagros (Najafi & Lajmorak, 2020), the offshore Morocco (Pichel et al., 2019; Uranga et al., 2022) or the North American Rocky Mountains foreland (Trudgill, 2011). The complexity that results from these mature, poly-phased systems makes it difficult to determine the tectono-stratigraphic history of the basin, especially in its early stages. For this reason, our current understanding of salt-influenced contractional systems has relied heavily on analogue and numerical modelling.

Highlights

- Shortening induced the African convergence toward Europe have been recorded within the central Algerian basin.
- Regional shortening was mainly accommodated by salt deformation, buckling the Messinian to present overburden.
- Two peaks of shortening are identified, with one at late Messinian and one at early to mid Plio-Quaternary.
- Salt tectonics along the Balearic margin is presently influenced by basement-involved extension/transtension.

The Mediterranean Salt Giant (MSG) is a relatively young wide and thick salt layer deposited during the latest Miocene (Messinian stage ca. 5.96–5.32 Ma, Krijgsman et al., 1999), at the convergence between the African and Eurasian plates. In the south-western Mediterranean sea, in the Algerian basin (Figure 1), the MSG was deposited in an already inverted system, after a short extensive rifting and drifting stage (ca. 8–6 Ma; Booth-Rea et al., 2007; Déverchère et al., 2005; Domzig et al., 2006; Mauffret et al., 2004; Rosenbaum et al., 2002; Serpelloni et al., 2007; Verges & Sabat, 1999). This implies that the salt system of the Algerian Basin evolved in a regional contractional setting since its deposition. It provides a unique opportunity to analyse contractional salt deformation during the early stages of shortening at the front of an incipient collisional fold-and-thrust belt.

The study area is located in the central Algerian Basin, in the south-western Mediterranean Sea. We investigate the salt deformation at the front of a recently inverted salt-bearing passive margin. A reprocessed pre-stack depth migrated 2D seismic reflection dataset allows us to examine the early spatial distribution of salt structures in a contractional system. We use structural maps of key horizons, thickness maps and stratigraphic relationships, in association with global gravity and magnetic maps, to investigate the relationship between salt morphologies, pre-salt segmentation and relief, distance from the active margin, and the variations in salt and overburden thickness.

2 | GEOLOGICAL SETTING

The Western Mediterranean Sea comprises a series of diachronous late Oligocene to Neogene (ca. 30–6 Ma)

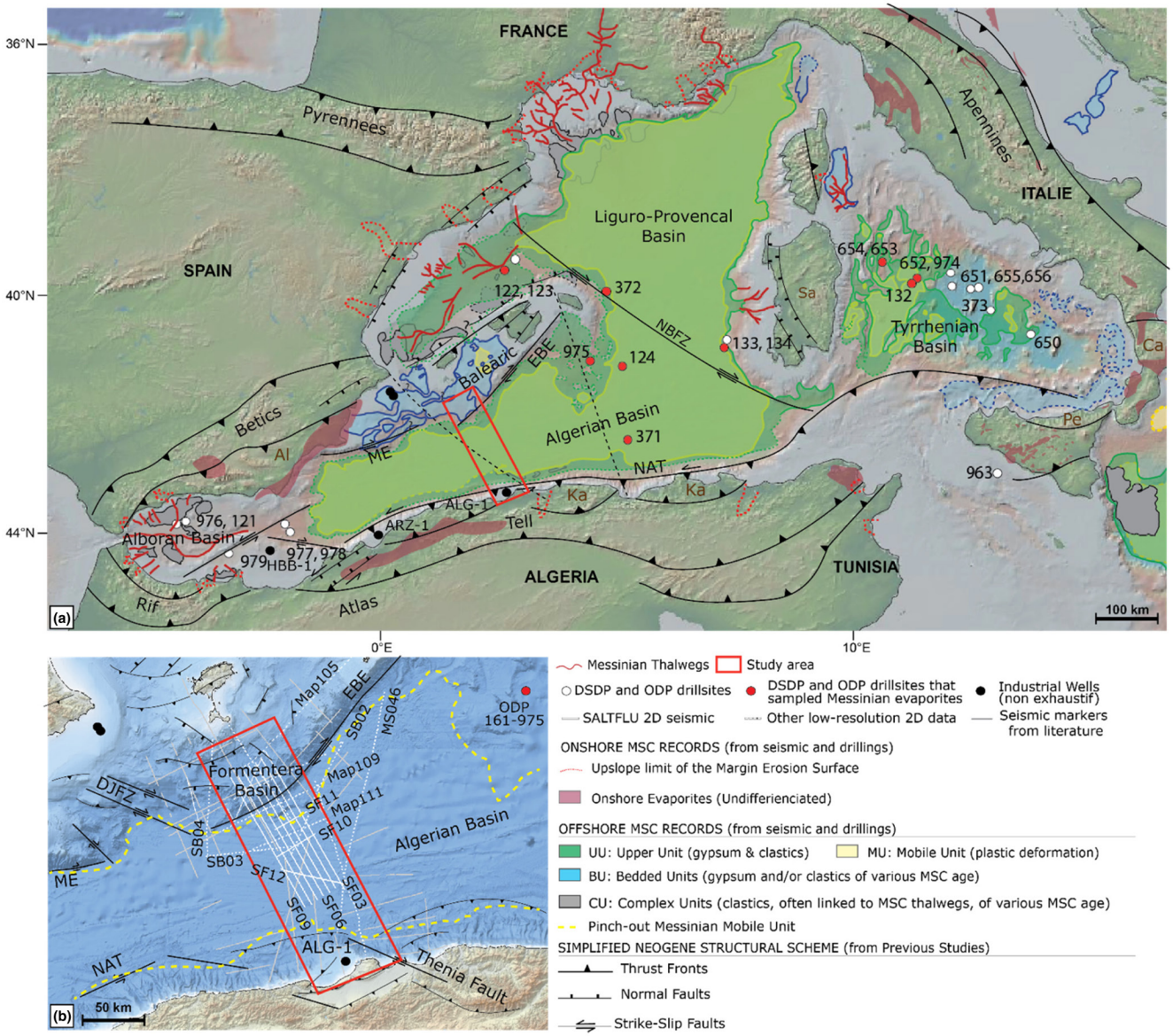

FIGURE 1 (a) Relief map of the Western Mediterranean sea (http://www.geomapapp.org; Ryan et al., 2009) with the present-day spatial extent of the MSC markers (modified from Lofi, 2018) and the general structural setting (modified from Arab et al., 2016; Etheve et al., 2016; Roure et al., 2014; Van Hinsbergen et al., 2014). (b) Relief map of the study area in the central Algerian basin (https://ows.emodnet-bathymetry.eu/wms) showing the location of seismic lines used in this study (2D data interpretations from literature refer to Bellucci, Pellen, et al., 2021), the pinch-out of the MU (Lofi, 2018) and the detailed structural setting (Acosta et al., 2013; Déverchère et al., 2005; Domzig et al., 2006; Driussi et al., 2015; 2016; Yelles et al., 2009). Ca, Calabria; DJFZ, Don Juan Fault Zone; DSDP, Deep Sea Drilling Program; EBE, Emile Baudot Escarpment; Ka, Kabylies; ME, Mazarron Escarpment; MSC, Messinian Salinity Crisis; NAT, North African Transforms; NBFZ, North Balearic Fault Zone; ODP, Ocean Drilling Program; Pe, Peloritan

back-arc basins that formed during the north-westward subduction of the Tethys ocean until the collision of Africa with Europe (Figure 1a; Gueguen et al., 1998; Jolivet et al., 2006; Rehault et al., 1984; Robertson & Grasso, 1995). The Algerian deep basin is situated in the south-western Mediterranean Sea, between the Balearic Islands (Spain) to the North and Algeria to the South (Figure 1a). Its northern and southern margins are marked by the transform zones of the Emile Baudot (EBE)—Mazarron (ME) escarpments and the North African transforms (NAT), respectively (Acosta et al., 2001; Booth-Rea et al., 2007; Mauffret et al., 2004). The EBE and ME escarpments are offset by the Don Juan Fault Zone (DJFZ; Acosta et al., 2013), which is interpreted by Vergés and Fernàndez (2012) as the north-western end of a dextral transform fault that runs until Algiers (Algeria), near the Thenia Fault on the conjugate Algerian margin (Figure 1b).

The basin inversion initiated during the Tortonian, with a general N-S to NW-SE shortening and sinistral

strike-slip movement (Déverchère et al., 2005; Rosenbaum et al., 2002; Stich et al., 2006; Verges & Sabat, 1999). After the inception of the Algerian margin inversion, during late Miocene (from ca. 5.97 to 5.33 Ma), the Messinian Salinity Crisis (MSC) led to the deposition of the MSG (CIESM, 2008; Hsü et al., 1973; Krijgsman et al., 1999; Manzi et al., 2013), resulting in the deposition of 500 m to 1.5 km of salt in the western Algerian basin (Haq et al., 2020). During the Plio-Quaternary, significant tectonic shortening along the Algerian margin generated a set of north-verging transpressional underthrust fronts, combining thin-skinned and thick-skinned tectonic styles (Déverchère et al., 2005; Domzig et al., 2006; Frizon de Lamotte et al., 2000; Leprêtre, 2012; Recanati et al., 2019; Leffondré et al., 2021; Strzerzynski et al., 2021). These thrusts likely signal early-stage subduction of the Algerian oceanic crust below Africa (Billi et al., 2011; Gueguen et al., 1998; Hamai et al., 2018; Leffondré et al., 2021; Recanati et al., 2019; Roure et al., 2012).

GPS-derived velocities show that today, the displacement rate increases westward but is highly variable laterally, with an average shortening of $1.5 \pm 0.5\,\mathrm{mm\,year^{-1}}$ at the central Algerian Basin (Bougrine et al., 2019; Serpelloni et al., 2007). North-westward Nubia-Eurasia plate motion has been shown to be relatively steady during the past ~13 Myr (DeMets et al., 2015). Assuming a constant rate of shortening since the onset of the MSC, the Algerian Basin should have accommodated approximately 8 km of shortening. For the Algerian margin and the coastal domains at the Algiers longitude, Strzerzynski et al. (2021) proposed a higher cumulated crustal shortening of 11 ± 3 km since the Pliocene.

Despite this, contractional deformation features have rarely been described in the Algerian Basin. Previous studies concluded that thin-skinned deformation started in the late Messinian, with a peak during the Early Pliocene, driven by salt-detached gravity spreading and gliding along a gently dipping base-salt surface (Dal Cin et al., 2016; Mocnik et al., 2014; Wardell et al., 2014). They suggested that the development of salt structures was controlled by the availability of salt and by the steepening of the base-salt due to the basin's thermal subsidence and the sedimentary loading. However, Camerlenghi et al. (2009) described salt-cored anticlines and pillows that lie too far from the continental slope of either side of the Algerian basin to be generated by the compressional stress induced by gravity gliding. They suggested they were tectonically-driven, either by underlying extensional or strike–slip faults, or by northward propagation of the compressional stress identified along the Algerian margin. Soto et al. (2019) also described contractional salt structures adjacent to the Algerian margin driven by the thick-skinned, tectonically driven shortening. They suggest that the Messinian salt layer acts as a décollement accommodating part of the thick-skinned shortening via thin-skinned diapir squeezing and folding, above a partially inverted half-grabens in the pre-salt sequence.

3 | DATASET AND METHOD

This study uses several 2D time-processed multichannel seismic reflection datasets acquired over the central Algerian Basin. The interpretation is focused on the Eurofleets project 'Salt deformation and sub-salt Fluid circulation' (SALTFLU) dataset, acquired in 2012 by the R/V OGS-Explora and recently re-processed in time and depth using the software REVEAL® by Shearwater Geoservices® (Blondel et al., in prep). Velocities used for the migration were estimated via ray-based tomography during the depth imaging processing. The maximum resolution varies from 7 to 80 m downward from the seabed to the pre-salt, with interval velocities ranging from 1511 to 5000 m/s, and a dominant frequency ranging from 15 to 55 Hz. The streamer was 3 km long, with a source consisting of two groups of four 210 cubic inch GI guns (the base-salt target in the abyssal basin was estimated at about 5 km below sea-level).

Other datasets used in this study consist of low-resolution seismic reflection data provided by the Instituto Geologico y Minero de Espana (IGME) and by the National Institute of Oceanography and Applied Geophysics (OGS). The processing flow applied to these data is not always known and their vertical resolution is at least 10 m. World gravity (Bonvalot et al., 2012) and magnetic anomaly maps (Meyer et al., 2017) were also used during the interpretation. All data are displayed with the Society of Exploration Geophysicists (SEG) 'normal' polarity convention, where a downward increase in acoustic impedance is represented by a positive reflection (yellow to red).

The interpretation of the seismic profiles was performed using the software Petrel® by Schlumberger®. Mapped seismic units are characterized by their seismic facies and seismic-stratigraphic relationships (as described in the following section). Terminology for the Messinian seismic units is derived from Camerlenghi et al. (2018), in the atlas of the "Seismic Markers of the Messinian Salinity Crisis" from Lofi (2018), including: the Upper Unit (UU), the Mobile Unit (MU) and the Lower Unit (LU). In the intermediate depth Formentera Basin and the EBE, two other units are defined: the Bedded Units (BUs) and the Complex Units (CUs). In this study, these two units are not described further and are assimilated to the UU (see Driussi et al., 2015; Raad et al., 2021).

Mapping is performed in the time domain because only the SALTFLU data has been processed in depth. As the

Seismic unit	Interval velocity (m/s)
Water column	1530
Plio-Quaternary (seabed to top UU/MU)	$1600+1.5(\lvert z-z_0\rvert)$
Messinian Upper Unit (top UU to top MU)	$2500+0.6(\lvert z-z_0\rvert)$
Messinian Mobile Unit (from top to base MU)	4300
Pre-Evaporitic Unit (from base salt)	$2700+1.2(\lvert z-z_0\rvert)$

Note: The velocities are based on the velocity models obtained from the depth processing of the SALTFLU dataset.

TABLE 1 Interval seismic velocities used for the time to depth conversion of the seismic surfaces

interpretation is based on 2D seismic data, the steep flanks of the diapirs are not well imaged, particularly where overhanging salt is present. Out-of-plane reflections may also be present in the 2D seismic sections presented. The spacing of the 2D lines is sparse with respect to the 3D geometry of salt structures, which may change abruptly over short distances. This makes the interpolation of the top salt surface between lines challenging. To aid the interpolation, the structural trends of bathymetric features observed on the seabed are used to guide the subsurface interpretation between lines (Figure 4a). Time surfaces are then converted to depth based on the velocity gradients obtained through the depth imaging of the SALTFLU data. The parameters used for the conversion from time to depth are presented in Table 1. Seismic markers published by (Bellucci, Pellen, et al., 2021) are also included as input for computing the isochore maps.

4 | RESULTS

4.1 | Seismic facies

Seven horizons defining six seismic units have been mapped across the study area (Figure 2). From oldest (deepest) to youngest (shallowest) the mapped units comprise: the Pre-salt unit, the Mobile Salt Unit (MU), the Upper Unit (UU), the lower Plio-Quaternary unit (PQ1), the middle Plio-Quaternary unit (PQ2) and the upper Plio-Quaternary unit (PQ3).

4.1.1 | Pre-salt unit

The pre-salt unit is the oldest and deepest mapped seismic unit. It comprises low amplitude and low frequency reflections, apparently continuous but generally poorly imaged (Figure 2). The pre-salt is best imaged along the basin margins (Figure 2a), where it is fan-shaped and onlaps the acoustic basement (interpreted as the post-rift unconformity). The unit is thickest along the Algerian Basin margin to the south (700 to 900 m), where the base is observed down to ca. 5.8 km below sea-level (Figures 3 and 4b). Previous studies by Leprêtre (2012) and Medaouri et al. (2014) associated the pre-salt unit with grey plastic marls, middle to late Miocene in age, drilled in the wells Algers-1 (ALG-1) and Arzew-1 (ARZ-1), on the Algerian shelf (Burollet et al., 1978).

4.1.2 | Mobile Salt Unit

The highly deformed MU overlies the pre-salt unit. It is characterized by semi-transparent and chaotic seismic facies (Figure 2). The upper MU exhibits low frequency and low amplitude internal reflections, particularly toward its top, making recognition of the top salt difficult. Locally, it forms diapiric structures and can appear at an allochthonous stratigraphic level (Figure 3). The regional base-salt is defined by a strong soft-kick in the deep basin. There is little to no evidence supporting the presence of the LU described by Lofi (2018) in the study area (Figure 2). A maximum salt thickness of 1.8 km is observed within the diapirs in the deepest part of the basin, while its average thickness is estimated around 600 to 800 m (Figure 5a). The unit thins toward the margins of the basin where it pinches out (Figures 3 and 6). No wells have ever been drilled through the MU in the Algerian basin. However, its seismic facies and diapiric geometries are characteristic of dominant halite composition and dirty salts (Medaouri et al., 2014).

4.1.3 | Upper Unit

The UU is characterized by a continuous, stratified, divergent seismic facies with high amplitude and high to medium frequency reflections. The overall amplitude and frequency of the reflections decrease with depth (Figure 2). The UU reflections onlap the underlying MU within the basin, and the pre-salt unit along the margins where the MU is absent (Figure 3). The contact between the UU and MU is poorly defined due to: (i) the lithological transition is gradational, (ii) the edges of the complex structures formed by the deformed MU are poorly

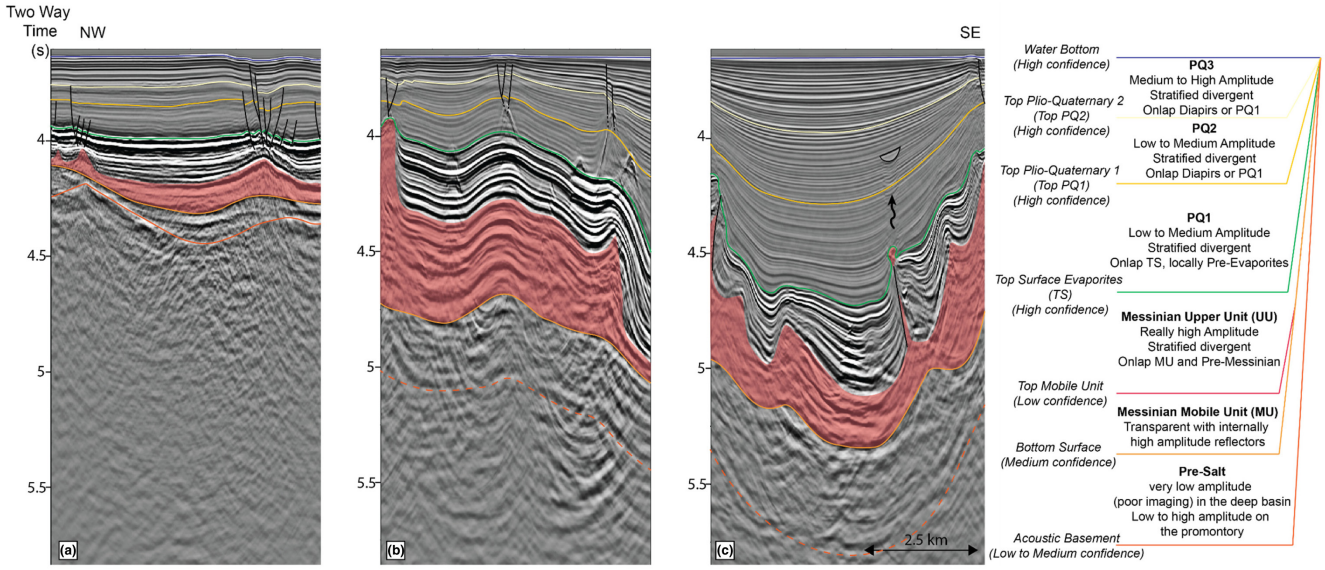

FIGURE 2 Seismic horizons interpreted within the deep Algerian basin along the seismic line SALTFLU 08. (a) Seismic profile 18 km southeast of the EBE illustrating a salt-cored anticline/pillow, with its faulted overburden (UU + PQ 1–3 units) and a landward dipping pre-salt; (b) seismic profile 40 km southeast of the EBE illustrating wider salt-cored anticlines/pillows, with faulted overburden that thickens between salt structures (c) seismic profile 80 km southeast of the EBE, 34 km from the North African escarpment, with salt diapirs piercing up to TOP PQ1 associated with amplitude anomalies and pull-downs, suggesting the presence of gas chimneys (indicated by a wiggling arrow on c)

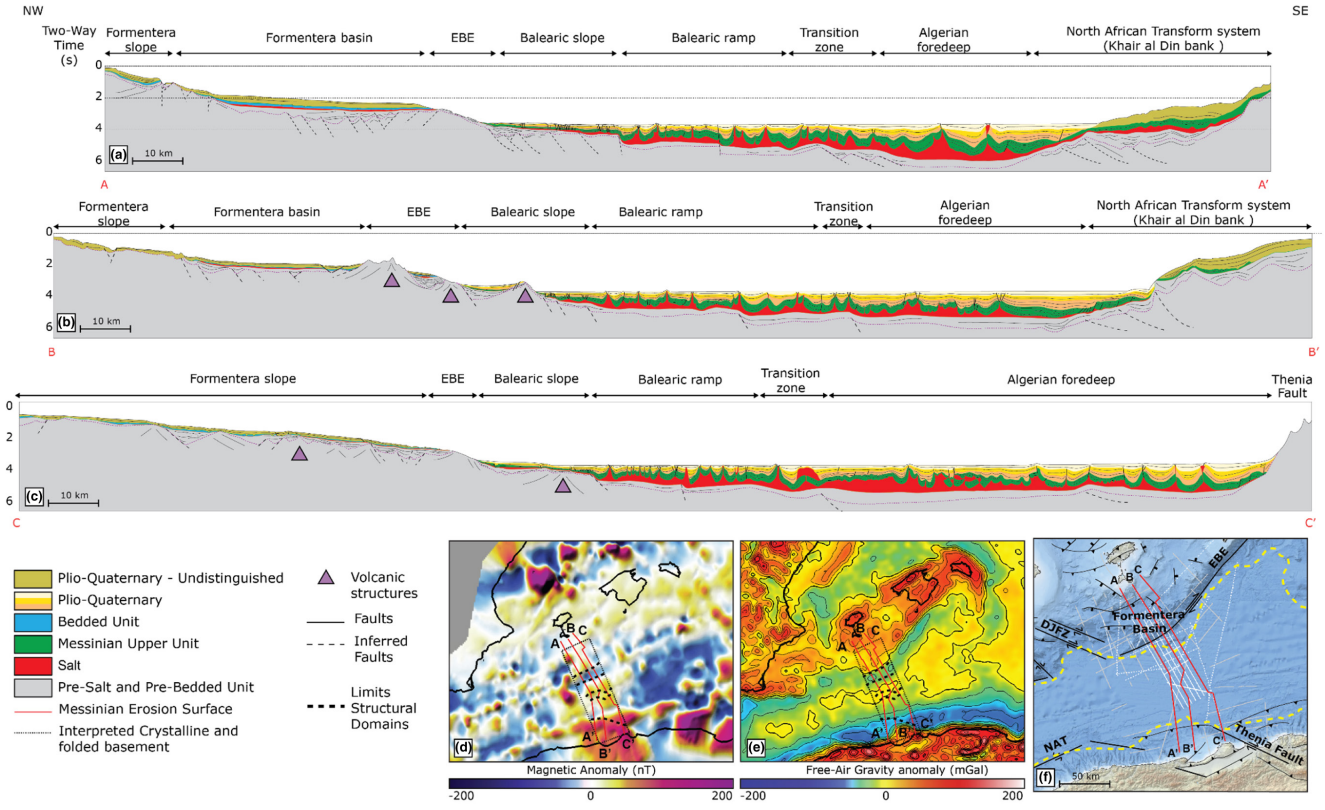

FIGURE 3 Schematic cross sections from the Balearic margin to the North African margin. To the west (a and b), the Algerian basin is narrower, the Emile Baudot escarpment is faulted, the Balearic slope uplifted, and the North African transform (NAT) is marked by thick-skinned thrust fronts. To the east (c), the Algerian basin is wider, the Emile-Baudot is less steep but the Algerian margin is more abrupt, without visible thrust fronts. The salt deformation appears more intense in the east, with several allochthonous salt sheets. The base-salt is not flat throughout the whole basin, with marked base-salt steps along the Balearic slope and the transition zone. This drop is aligned along WSW-ENE positive gravimetric (Bonvalot et al., 2012) and magnetic anomalies (Meyer et al., 2017)

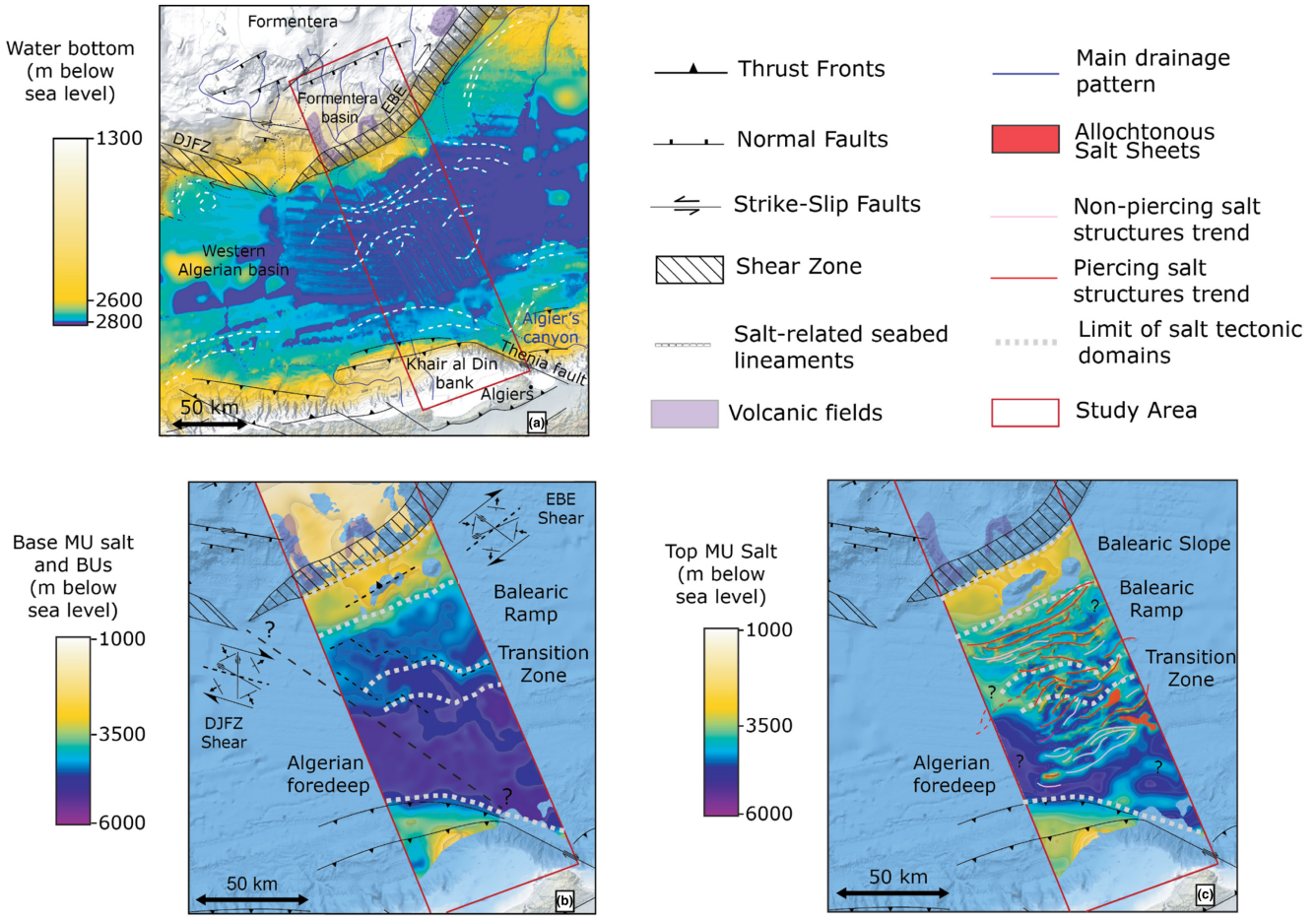

FIGURE 4 Depth maps from the sea level of (a) the seabed with key structural features (modified from Acosta et al., 2013; Domzig et al., 2006) and interpreted salt-related deformation trends, (b) the top salt with interpreted salt-related structural trends and (c) the base-salt with interpreted structural trends. Dashed lines show the limits of the main structural domains (see text). Background bathymetry from https://ows.emodnet-bathymetry.eu/wms

imaged by 2D seismic data, and (iii) internal multiples of the UU interfere with the potential presence of intra-salt reflectors. The base of the UU is therefore defined as the youngest continuous high amplitude reflection onto which the UU reflections onlap. At the top, the unit is bounded by a continuous high amplitude reflection that strongly contrasts with the overlying unit, whether it is a hard or a soft kick.

The deformation of the UU is concordant with the underlying MU, although locally truncated by it where diapiric structures penetrate the overburden (Figure 6). The average thickness of the UU is about 400 m. It thins across the structures formed by the MU, with an observed maximum of 600 m between salt diapirs (Figure 5b). It thins toward the basin margins where it pinches out (Figure 3). Based on scientific wells that penetrated the uppermost UU in the Algerian Basin (ODP-975, DSDP-124, DSDP-371), it is thought to comprise evaporites such as dolomites, gypsum and anhydrite, interbedded with mud and marls, and possibly rich in organic matter (Comas et al., 1996; Hsu et al., 1978; Ryan et al., 1973).

4.1.4 | Plio-Quaternary overburden

The Plio-Quaternary overburden is divided into 3 sub-units of similar seismic frequency but with different amplitudes. It locally onlaps the underlying UU, the basement or the allochthonous MU (Figures 2 and 6). The deepest Plio-Quaternary sub-unit, PQ1, is characterized by a low to medium amplitude and high frequency seismic facies, with continuous, divergent reflections. The overlying PQ2 displays a similar facies, but with slightly higher amplitude reflections. The contact between PQ1 and PQ2 is defined by a regional high amplitude and low frequency soft kick (TOP PQ1), onto which the PQ2 reflections onlap.

The youngest and shallowest sub-unit, PQ3, is comparable and conformable with the PQ2 facies, but with much higher amplitude reflections (Figure 2). The contact between PQ2 and PQ3 is defined by a regional high amplitude and low frequency reflection (TOP PQ2), which marks the contrasting amplitudes between PQ2 and PQ3.

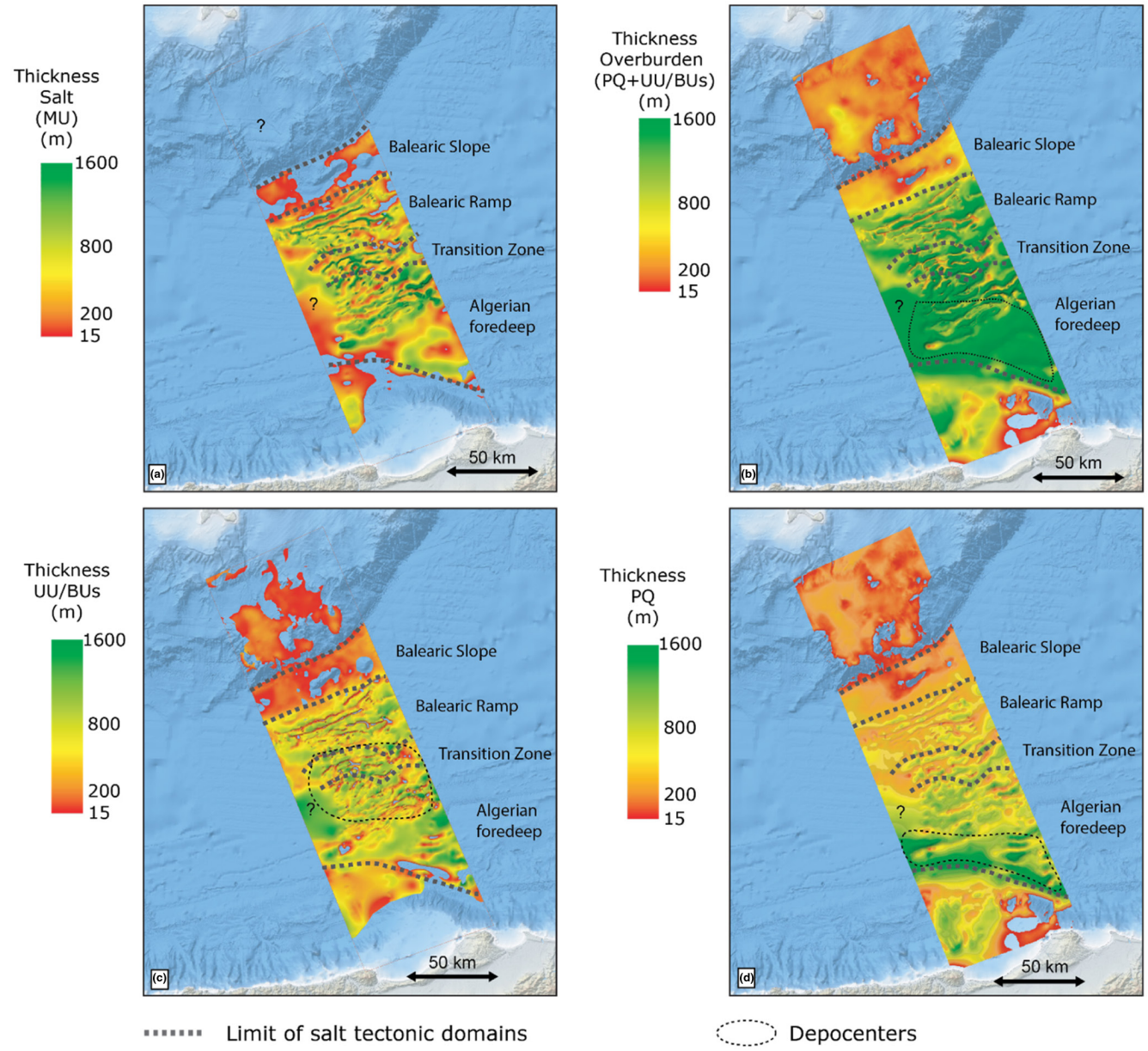

FIGURE 5 Thickness maps of (a) the salt unit, (b) the total overburden (PQs + UU + BUs), (c) the Upper Unit (UU + BUs) and (d) the Plio-Quaternary (PQ). These maps show an asymmetric distribution of the overburden with thickest deposits along the North African thrust front during the Plio-Quaternary. Dashed lines show the limits of the main structural domains (see text). The base-salt map reveals the base-salt relief with structural trends parallel to the synthetic and antithetic conjugate faults of the EBE shear zone. DJFZ, Don Juan Fault Zone; EBE, Emile Baudot Escarpment. Background bathymetry from https://ows.emodnet-bathymetry.eu/wms

Along the basin margins, PQ3 directly onlaps TOP PQ1 or the TOP Evaporites.

The thickness of the Plio-Quaternary unit shows an asymmetrical distribution, with the main depocenter along the southern Algerian margin (up to 1.4 km; Figures 3 and 5d). Its thickness is influenced locally by the salt structures, with local maxima in between salt highs. The lithology of the Plio-Quaternary unit is inferred from scientific wells in the Algerian Basin, where it consists of pelagic oozes with sandy intercalations with a downward increasing carbonate content (Comas et al., 1996; Hsu et al., 1978; Ryan et al., 1973). Although these wells are located more than 100 km away from the study area, they are assumed to be deposited in a similar deep-water setting, where the sedimentary record should be comparable at a basin scale.

4.2 | Interpreted structural domains

We define five structural domains in the deep Algerian Basin, classified according to the thickness of the overburden (UU + PQ units), the thickness of the salt,

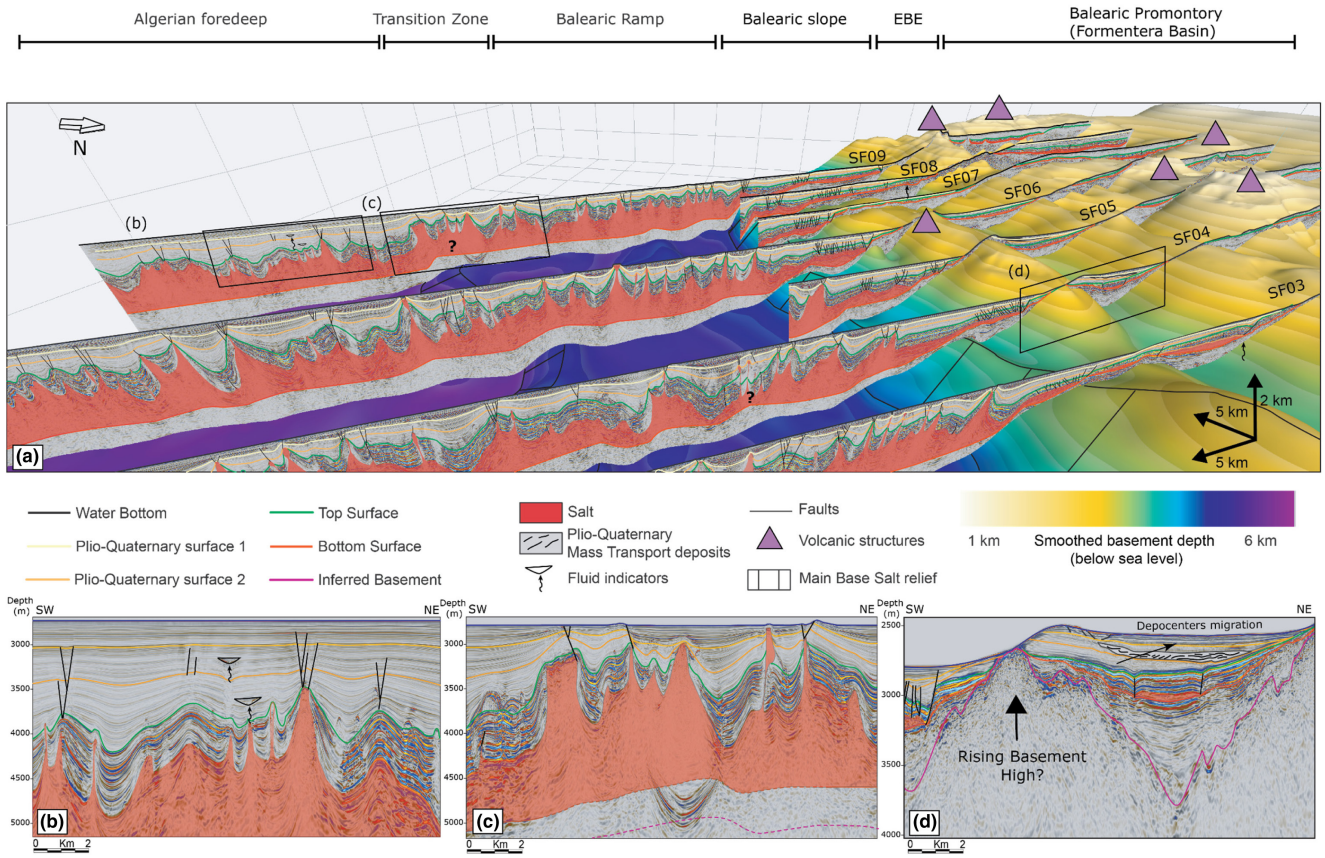

FIGURE 6 (a) 3D view of the interpreted basement along the north-western Balearic margin and interpreted SALTFLU 2D seismic sections. The basin is divided into five structural domains based on the thickness of the overburden, the thickness of the salt (i.e. MU), the base-salt relief and the style of the salt structures. The NE–SW trending Emile-Baudot escarpment is bordering the northern margin of the Algerian basin, with at least two volcanic pinnacles groups (presumably early Pleistocene to recent, according nearby dating performed by Acosta et al., 2004). (b) Zoom on line SF09, in the Algerian foredeep, where wiggling arrows indicate areas of amplitude blanking, amplitude anomalies, pull-downs and/or disturbed bedding, representing possible fluid migration pathways. (c) Zoom on line SF10, in the Transition zone. (d) Zoom on line SF04, in the Balearic slope, where a NE–SW trending topographic high is dividing the deep Balearic slope in two, with Plio-Quaternary mass transport deposits on its landward north-western flank

the base-salt relief and the type of salt structures observed. From the northern margin moving south we distinguish: (i) the deep Balearic slope, (ii) the Balearic ramp, (iii) the transition zone, (iv) the Algerian foredeep, and (v) the North African thrust front (Figures 3, 4, and 6).

4.2.1 | Balearic slope

The Balearic slope domain is bordered by the EBE to the northwest and a 500 m base-salt step to the southeast (Figure 6a). It is internally segmented by a local topographic basement high that separates two gently landward-dipping ramps (Figure 3b, Figure 6d). In this domain the overburden is relatively thin (up to 700 m) with a broadly uniform thickness. Likewise, the thickness of the salt remains broadly constant and below 300 m. The salt pinches-out against the topographic high or the EBE, with small salt-detached normal faults and associated rollovers at its edges (Figures 6 and 7a).

The salt-detached deformation in this domain is characterized by salt anticlines/pillows with a relatively small vertical amplitude (<150 m) and a short wavelength (1 to 2 km) (SP1, SP2 in Figure 7a). The crests of the structures are populated with small normal faults (Figure 2). Most faults terminate at TOP PQ1, but some also penetrate up to PQ2, PQ3 and the seabed (Figure 7a). Within the perched basin between the EBE and the basement high, depocenters progressively migrate away from the basement high from the pre-salt unit to PQ3 (Figure 6d), with locally chaotic intervals that are interpreted to represent Mass Transport Deposits (MTDs).

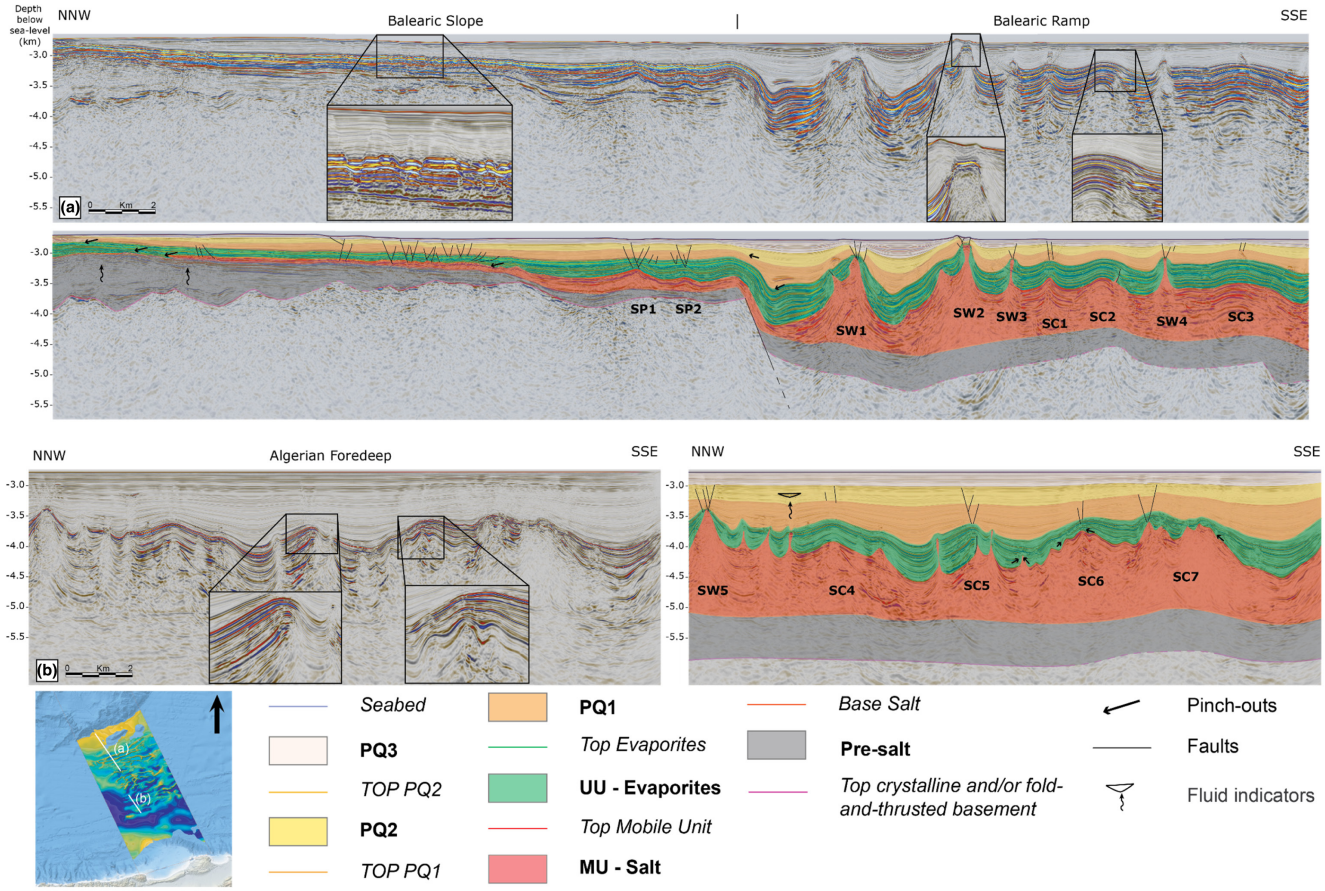

FIGURE 7 Dip-oriented seismic profiles showing non-piercing salt structures (anticlines as SCs, salt pillows as SPs, salt walls as SWs) in the northern Balearic margin (a; SF08) and in the Algerian foredeep (b; SF09). Location map shows the top salt from Figure 4b. Vertical exaggeration ×2

4.2.2 | Balearic ramp

The Balearic ramp extends from the previously described base-salt step at the end of the Balearic slope, to a zone of complex and poorly imaged salt structures where another base-salt step has been identified (Figure 6). In this domain the base-salt is mainly flat or landward dipping, and maintains a relatively constant depth of 4500 m below sea level (Figures 7a and 8a). The overburden here is significantly thicker, up to 1.7 km between salt structures, half of which is UU and half PQ.

The salt is also thicker and more deformed than on the Balearic slope, with an average thickness of 800 m and a local maxima up to 1.5 km within diapirs (Figures 7a and 8a). Salt anticlines are common and larger, with medium to high amplitudes (250 to 600 m) and medium to long wavelengths (1.5 to 3 km). They seem to be aligned along an arcuate ENE-WSW trend, parallel to the EBE (Figure 4b).

Diapiric structures are common, notably at the base of the Balearic slope step. They generally reach to the TOP PQ1 seismic horizon, with a PQ2-PQ3 roof (SW2 in Figure 7a and "SW1", "SW2", "SW3, "SW4" in Figure 8a). In some cases, they reach the seabed where they are locally extruded (SS1 in Figure 8a). Some diapirs are flat-topped ("SW2" in Figure 7a, "SS1" on Figure 8a). The UU to PQ1 units show minimal thickness variations with a relatively uniform thickness of 500 ± 100 m (Figures 7a and 8a). They are thining and strongly upturning (>45°) within ca. 300 m of the diapir contact, where the strata become thin or absent (<100 m). Wide (>10 km) and steep UU to PQ2 panels adjacent to squeezed diapirs are also present ("SW1" and "SW2" in Figure 7a, "SS1" in Figure 8a). Near the top of the diapirs, these upturned limbs are delimited by crestal normal faults. They are often observed at the borders of the Balearic margin (i.e. where the base salt drops), at the Balearic slope and the Transition zone. Two trends of salt walls can be distinguished (Figure 4c):

1. ENE-WSW trending salt walls located at the foot of the base-salt step, parallel to the EBE, that are expressed at the seabed by two belts of NE–SW elongated sea hills (Figure 4a, "SW1" and "SW2" on Figure 7a). They

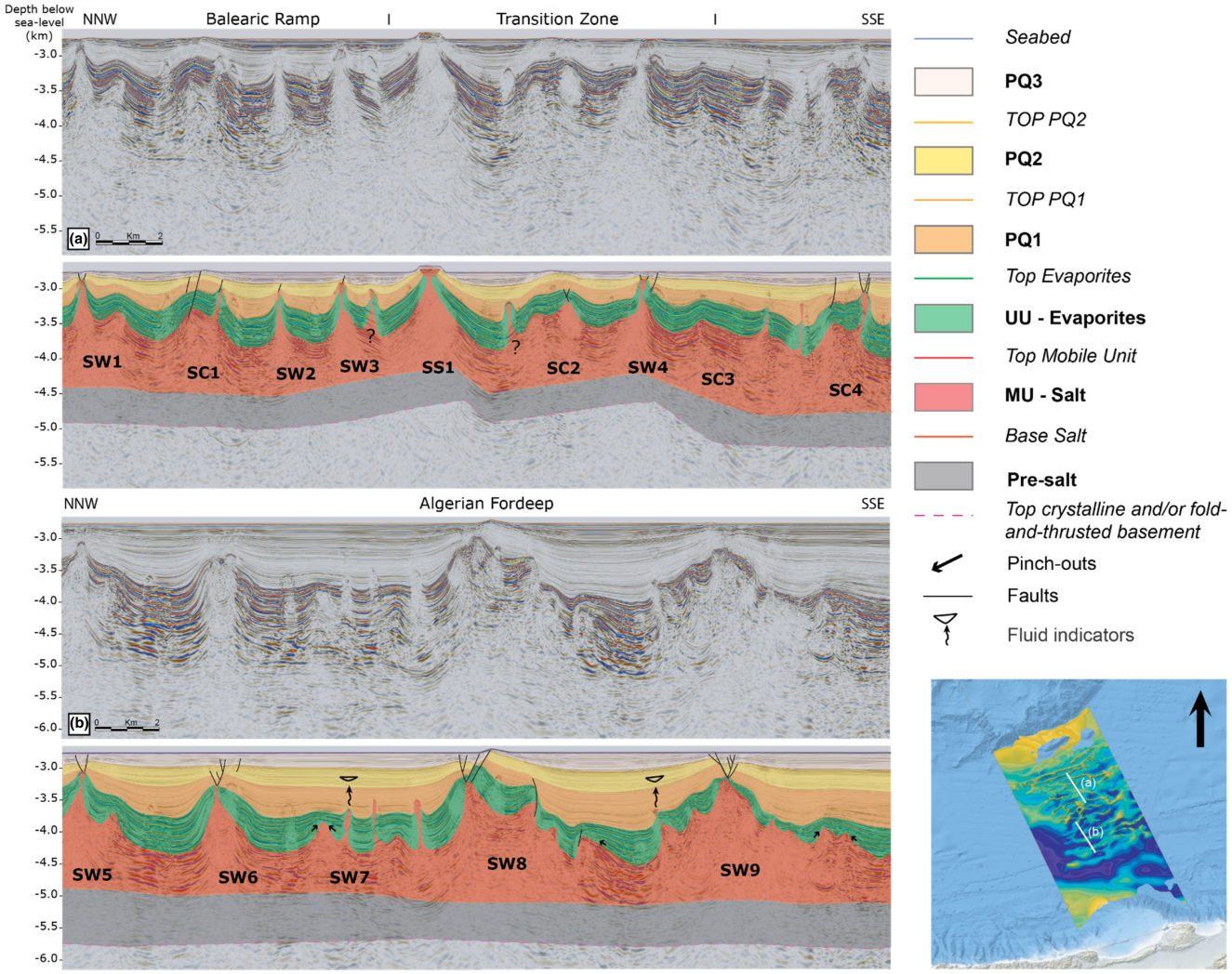

FIGURE 8 Dip-oriented seismic profiles showing piercing salt structures within the central Algerian basin (anticlines as SCs, salt walls as SWs, salt stocks as SS), in the northern Balearic margin (a; SF06) and in the foredeep of the Algerian basin (b; SF08). Most structures appear to be squeezed by a post-Messinian shortening episode that seems to be ongoing at present. The vertical flanks are not properly imaged by the 2D seismic data, particularly when the top of the diapirs is wider than its stem. SS1 is well imaged by several 2D seismic lines that allow us to discern it as a salt stock. Location map represents the top salt from Figure 4b. Vertical exaggeration ×2

display strongly rotated flanks, with inward-dipping salt-detached normal faults immediately above their crests. Most often the landward limb is slightly more upturned than the seaward limb, forming the sea hills observed on the seabed (Figure 4a) rather than the salt diapir itself ('SW2' in Figure 7a).

2. WNW-ESE trending salt walls (Figures 4 and 8a), generally associated with salt-detached faults above their crests. They typically appear to be squeezed, with a narrow diapir stem or secondary weld separating the head of the wall from its triangular shaped pedestal (Figure 8a, "SW2", "SW3", "SW4"). Locally, small salt-detached thrust faults seem to be present, but their offset are not well imaged to confirm their throw ("SC2" in Figure 7a). The PQ2 and PQ3 units thicken between these structures and drape their crests.

4.2.3 | Transition domain

The transition domain separates the Balearic ramp, where the base-salt stands at a depth of 4.5 km below sea level, from the Algerian foredeep, where salt stands a depth of 5 km below sea level (Figures 3c and 8a). In this domain the base-salt relief is generally poorly imaged due to the presence of large, complex salt structures, but generally presents a steep basinward slope. Salt structures are tall (up to 1.7 km) and squeezed (Figure 6a,c), with thick accumulations of Plio-Quaternary sediments (up to 2 km) in halokinetic mini-basins (ca. 1.5 to 3.5 km wide).

When a very weak signal is recorded below some structures, the presence of allochthonous salt sheets is suggested (Figure 9). The 4.5 km wide salt sheet SH1 lying above the UU is relatively well imaged (Figure 9a, SH1),

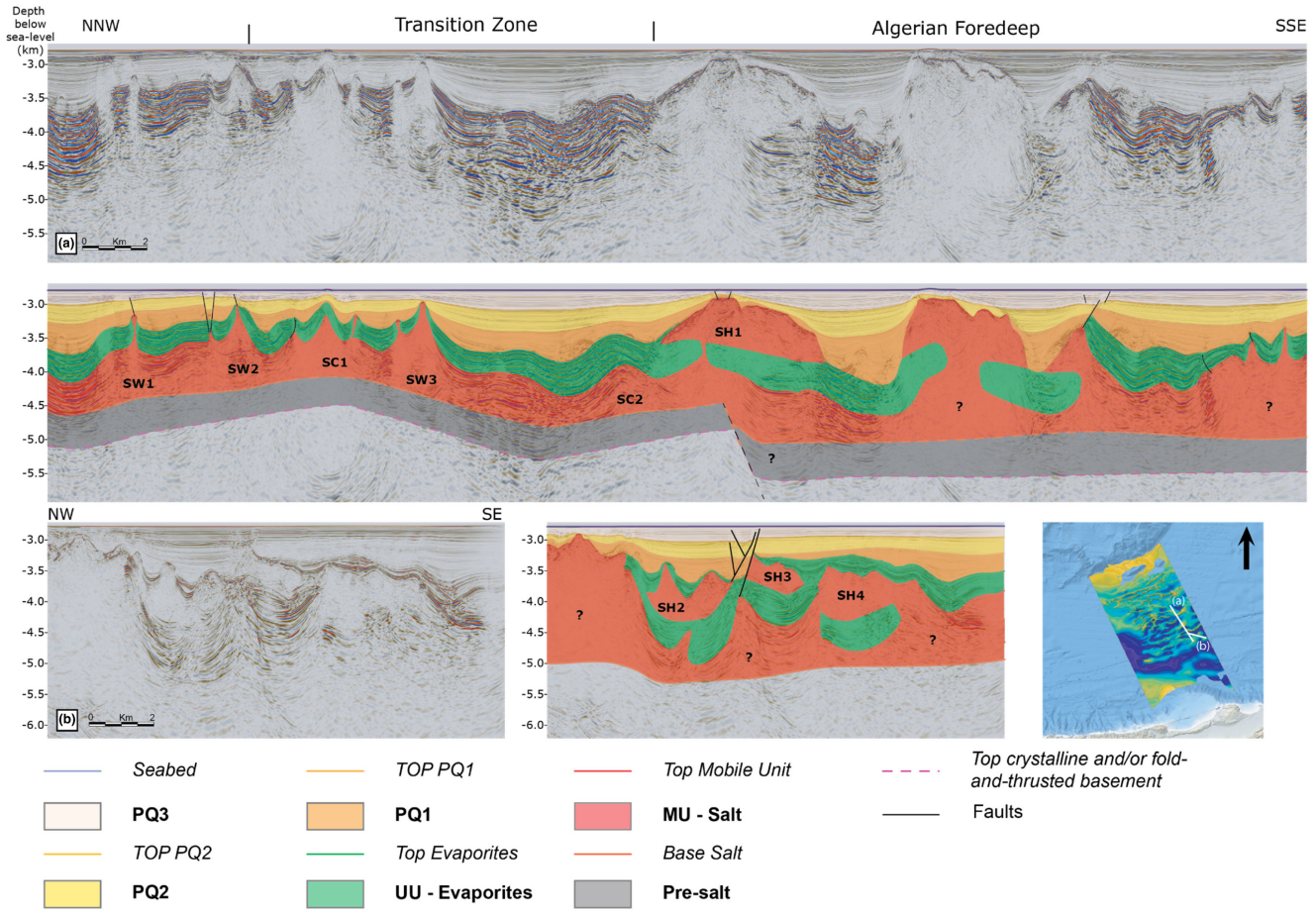

FIGURE 9 Seismic profiles showing salt sheets within the central Algerian basin (anticlines as SCs, salt walls as SWs, salt sheets as SH), in the foredeep of the Algerian basin along seismic profiles SF04 (a) and SF12 (b). Salt sheets are located in the Algerian foredeep and along the transitional slope. They are poorly imaged on the available 2D seismic data, with very limited signal below the salt. Some important transparent salt structures could potentially be salt sheets because internal reflections are overmigrated if flooded with salt (in this case the available data do not allow us to distinguish them from a wide piercing diapir). SH1 seems to be located above a faulted basement. Location map represents the top salt from Figure 4b. Vertical exaggeration ×2

with a salt stem connecting it to a triangular salt pedestal. The overburden is uplifted and faulted above the sheet, with moderately upturned strata. The PQ units onlap and thin across the sheet.

4.2.4 | The Algerian foredeep

The Algerian foredeep extends from the transition zone to the southern basin margin, bounded by the North African transform margin (Figures 3 and 4). In this domain the base-salt appears sub-horizontal, at a constant depth of 5 km below the sea level (Figures 3, 7b, and 8b). Contrary to the rest of the deep Algerian Basin, the pre-salt here displays a good signal-to-noise ratio, with flat parallel low-frequency and medium amplitude reflections suggesting either (i) a better penetration of the emitted seismic signal or (ii) stronger acoustic impedance contrasts, notably at the base of the pre-salt. The Plio-Quaternary is thickest in this domain (Figure 5c), where it makes up approximately 60% of the total overburden. Diapirs rarely penetrate or deform the PQ overburden or seabed in this domain, but they commonly penetrate the UU (Figures 6, 7b, and 8b). The UU reflections steepen toward and onlap the salt structures. In the south-western part of the study area, strong amplitude anomalies are observed within the PQ, with a dimming of the amplitude and a "pull-down" effect underneath (Figures 2c and 6b, above SW7 in Figure 8b).

Salt structures are aligned along an arcuate ENE-WSW trend, above a nearly flat-lying pre-salt (Figure 4). Salt anticlines display a large amplitude (400 to 800 m) and a medium to long wavelength (1.5 to 3.5 km; Figures 7b and 8b). The folding mainly affects the UU and lower PQ1, while the upper PQ1 and overlying units are relatively undeformed. Locally, at the top of the salt, shorter wavelength and lower amplitude polyharmonic folds are observed (SC6 to SC7 in Figure 7b), which are onlapped by UU reflectors. Diapiric salt structures are complex with squeezed salt walls and

minibasins uplifted above regional ("SW8" in Figure 8). Salt-detached thrust faults are locally observed between the salt structures (right-flank of "SW8" in Figure 8b, between "SC1" and "SW3" in Figure 9a). We observe an increased intensity of the salt-related deformation toward the north-eastern part of the study area, with wide allochthonous salt sheets within the UU and the early PQ (Figure 9).

5 | DISCUSSION

Since its deposition, the Messinian salt in the Algerian Basin has been in a basin under inversion, with thick-skinned thrusting and possible initiation of subduction of the Algerian oceanic crust beneath the North African margin (Frizon de Lamotte et al., 2000; Recanati et al., 2019; Strzerzynski et al., 2021). In this discussion, we assess how this shortening has been recorded by salt tectonics adjacent to the Algerian margin. We first discuss whether the development of salt structures in the previously described structural domains is predominantly driven by gravitational forces or by lateral forces related to regional tectonics, and how the dominant drivers vary through time and space. Secondly, we focus on the Balearic margin, speculating its influence on the salt tectonic system.

5.1 | Salt tectonics along the Balearic ramp

The stratal onlapping geometries of the UU to PQ1 units, with thinning and upturned strata in the vicinity of the diapirs, are characteristic features of halokinetic sequences deposited during near surface growth of load-driven passive diapirs (Jackson & Hudec, 2017; Rowan & Giles, 2021). This suggests that along the Balearic ramp, the early stage of the deformation was marked by load-driven passive diapirism, synchronous with deposition of the UU and early PQ1 sequences. Along the Balearic slope, where the salt thins and pinches out, normal faults record some extension in the overburden (Figures 6a and 7a). These faults show relatively small displacement, recording a minor gravity-gliding of the salt along its base (see Section 5.5). Furthermore, even though the pre-salt imaging is poor, the base salt relief is either flat or landward dipping, which would imply low basinward gravity gliding.

During the deposition of PQ1 the stratal geometries change. The thick UU-PQ1 strata are folded above salt-cored anticlines, elevating their roof above regional (Figure 6a). Most diapirs observed are squeezed in between UU to PQ1 rotated limbs. The TOP PQ1 horizon marks a regionally discordant surface which is onlapped by PQ2 strata. The wide steeply upturned limbs often observed at the borders of the Balearic margin (i.e. where the base salt drops) are interpreted as megaflaps (Rowan et al., 2016; Rowan & Giles, 2021). These features are commonly observed in contractional salt systems (Jackson & Hudec, 2017; Rowan & Giles, 2021). Because there is little evidence of gravity gliding, this contraction is interpreted to be tectonically driven.

We suggest the shortening initiated during PQ1 and peaked around TOP PQ1, generating the structures onto which the PQ2 strata onlap. The pre-existing passive diapirs were squeezed, and the overburden buckled, with PQ1 to PQ2 growth strata recording syn-shortening folding of the overburden. At the edges of the Balearic ramp, basement-involved normal faults (Figure 7a) and a rising basement high (Figure 6d) suggest the deformation is locally thick-skinned. Basinward, the pre-salt imaging is not good enough to discern whether the salt deformation involved the basement.

After Top PQ1, there seems to be a change in salt kinematics. Most diapirs do not rise above Top PQ1, and a PQ2-PQ3 roof is draping the diapirs crest (Figure 7). The burial of the diapirs results from the aggradation rate of the overburden out-competing the rise rate of the diapirs (Jackson & Hudec, 2017). This could be due to either an increase in sedimentation rate or decrease in the rate of diapiric rise. We suggest that the decreasing rise rate of the diapirs could be related to a diminishing regional shortening following the peak at Top PQ1, combined with an increased sediment supply from newly formed topography at the basin margin. This is also supported by growth strata above salt-cored anticlines: the PQ2 unit appears slightly folded, but the overlying PQ3 unit is relatively undeformed.

Though most become buried, some diapirs manage to continue rising actively and penetrate the younger PQ2-PQ3 units ("SW1" and "SW2" in Figure 7a). Recent crestal faults are present above the diapirs, with uplifted and upturned PQ2-PQ3 sequence at their flanks, suggesting ongoing active salt diapirism. At the foot of the base salt drop delineating the Balearic slope and the Balearic ramp, they form ENE-WSW trending salt walls, whose uplifted limbs form seahillson the current seabed (Figure 4a). At present the diapirism seems dominantly load-driven, with thick subsiding minibasins expelling salt into the precursor structures. Some salt-cored anticlines are also still inflating, arching their overburden ("SC1" in Figure 8a). Passive diapirism resumes locally where the overburden is not too thick ("SS1" in Figure 8a).

5.2 | Salt tectonics along the Algerian foredeep

In the Algerian foredeep, the UU to PQ1 interval is not as uniformly distributed. Short wavelength buckle folds at the

base of the UU suggest an early UU phase of contraction ("SC6" in Figure 7b, "SW9" in Figure 8b). It is not clear whether this contraction was driven by thick-skinned, tectonic shortening or local thin-skinned, gravitational instability. Early thin-skinned, gravitational salt deformation during deposition of the UU is observed on other Western Mediterranean margins, such as in the Gulf of Lion (Bellucci, Aslanian, et al., 2021; Mianaekere & Adam, 2020), the Western Sardinian (Del Ben et al., 2018), but also along the Levant margin in the eastern Mediterranean (Gvirtzman et al., 2013). The small magnitude of the folds and the analogy with other Mediterranean passive margins lead us to favour the gravity-driven interpretation, with salt spreading and gliding on a tilted margin. The development of thick-skinned thrust faults along the inverted Algerian margin could have played a role in steepening the base salt.

The upper UU onlaps these precursor contractional folds and shows considerable thickening between diapiric salt structures (Figures 7b and 8b), suggesting a higher rate of syn-depositional subsidence and diapir rise than along the Balearic ramp at the UU stage. The salt diapirs are sparse and squeezed, with crestal faulting ("SC5" in Figures 7b and 8b) and strongly upturned flaps of UU to early PQ1 strata within ca. 300 m of the diapirs (e.g. "SW7" in Figure 8b). Generally, they do not penetrate strata younger than early PQ1, particularly in the western part of the study area (Figure 7b). They are interpreted as passive diapirs during UU deposition, which were then squeezed at the late UU-early PQ1 stage. The squeezing formed secondary wells that progressively disconnected the head of many diapirs from the salt source, inhibiting further rise. Similarly with the Balearic ramp, the squeezing is interpreted to be linked to a regional shortening episode. This event also generated large (up to 10 km) and widely spaced (3 to 8 km) salt-cored anticlines (Figures 7b, 8b and 9a), overprinting the previously mentioned early UU short wavelength folds.

In the north-eastern part of the Algerian foredeep, this early PQ1 shortening resulted in the extrusion of salt sheets emplaced above the UU (Figure 9). Locally, minibasins were shunted into each other and salt was squeezed out into allochthonous extrusions. With continued shortening, some of the salt extrusions coalesced into a canopy, with local secondary diapirism as the new salt layer is loaded by sediments (Figure 9b, "SH3", "SH4").

Along the Algerian margin, south of the Algerian foredeep, this quaternary shortening is thick-skinned, with north-verging thrust ramps delineating uplifted perched (piggyback) basins (Figure 3; Déverchère et al., 2005; Yelles et al., 2009; Leprêtre et al., 2013; Leffondré et al., 2021; Strzerzynski et al., 2021). Salt structures adjacent to the margin are squeezed and the whole overburden is folded in response to regional shortening, whereas the pre-salt sequence still preserves extensional half-grabens (Soto et al., 2019).

Following this early PQ1 contractional episode, the salt deformation decreases. To the south-eastern part of the study area, the early PQ1 is drape folding slowly rising salt structures and thickening into wide minibasins. The aggradation rate of the PQ sequences soon overtakes the rate of diapir rise and buries them under a thick roof. Crestal faults extend up to the TOP PQ2, indicating some persisting salt movement, but the late PQ1 to PQ3 units are deposited sub-horizontally.

Locally, active salt diapirs are still rising today, uplifting their very thick (1 km) roof 800 meters above regional ("SW8" in Figure 8b), and forming bathymetric highs on the seabed (Figure 4a). To the north-western part of Algerian foredeep, the salt sheets emplaced during the PQ1 shortening are still sourced at the autochtonous level and continue to inflate syndepositionally with the PQ sequences aggradation (Figure 9a). Their inflation is interpreted to be load-driven, with expulsion of the salt beneath the thick and wide (>1.5 km) subsiding minibasins. The influence of a steady but mild regional shortening is not excluded, in response to the current slow-rate crustal shortening at the Africa-Eurasia plate boundary (Bougrine et al., 2019). Locally, the presence of long subvertical faults and abrupt thickness variations within the PQ sequence (e.g. Figure 6a, along SF06 in the Transition zone) could potentially record a transpressional regime.

5.3 | Outward shifting of the contractional deformation during the Plio-Quaternary

We have shown that the regional shortening due to the ongoing inversion at the Algerian margin has been recorded within the central Algerian Basin. Most of the shortening is accommodated by the salt and the deformation of its roof. The salt acts as a decollement within the central Algerian Basin, allowing northward propagation of the contractional deformation, from the Algerian margin to the Balearic margin. We distinguish two stages of contraction:

1. First, a short late Messinian episode (MSC Stage 3), synchronous with the UU deposition, that was localized along the Algerian foredeep. This episode is interpreted as gravity-driven, related to thrust faults that steepened the base-salt at the toe of the Algerian margin fold-and-thrust belt.
2. The second episode, longer and more widespread, occurred during the PQ1-PQ2 deposition. This regional shortening accommodated northward propagation

of the Algerian deformation front, and its effects are diachronous across the basin. Along the Algerian foredeep, this shortening peaked during early PQ1. It resulted in high amplitude and widely spaced folds, with squeezing of pre-existing passive diapirs and extrusion of salt sheets. This contrasts with the Balearic ramp domain, where shortening peaked later, during latest PQ1. Precursor structures were squeezed with asymmetrical limbs tilted and uplifted. This second peak of salt deformation could be linked to the second phase of Atlas inversion (Pliocene to lower Quaternary) and the related Tell shortening that could have been recorded through the whole Algerian Basin, with notably the initiation of the north-verging thrusts at the toe of the Algerian margin (Frizon de Lamotte et al., 2000; Roure et al., 2012; Strzerzynski et al., 2021). The second episode is thick-skinned along the Algerian margin and could also reactivate more distal faults along the Balearic margin (see Section 5.5). In between these contractional pulses, the diapirism was mostly passive, driven by sediment-loading.

The decreased intensity of the salt-related deformation in the Algerian foredeep compared to the Balearic ramp during the Plio-Quaternary could be related to the higher sedimentation rate in the Algerian foredeep (more than 1 km on average within ca. 5.3 Ma). The rate of sediment aggradation during PQ1 outpaces the rate of diapiric rise in the Algerian foredeep (the thickness of the PQ1 unit doubles from the Balearic ramp to the Algerian foredeep), resulting in burial of the diapirs beneath a strong overburden. The thicker, stronger overburden also results in propagation of the contractional stresses further out into the basin (on the Balearic ramp) along the salt decollement, where the strain is accommodated by folding of the thinner overburden and squeezing of pre-existing diapirs.

Salt decollement facilitated the sliding and folding of the overburden, hereby accommodating the stress applied by the ongoing shortening. Basinward propagation of the contractional stresses allowed a wide thin-skinned deformation with a focused folding out into the foreland, similarly with the Appalachian Plateau, the Franklin Mountains in north-western Canada, and the Jura of the Alps (Davis & Engelder, 1985). During the Plio-Quaternary, the thicker overburden of the Algerian foredeep, adjacent to the thrust front, can translate without deforming by sliding on the salt. The deformation is instead focused outward, to the Balearic side, where the overburden is weaker. Base-salt relief along the transition zone and the Balearic slope may be able to disrupt this gliding, resulting in a highly deformed overburden (Figures 6c and 9). The poor imaging along the Transition zone do not allow use to confidently interpret the amplitude and the influence of the base salt relief there.

5.4 | Lateral variability in the complexity of salt structures and magnitude of deformation

In the Algerian foredeep, we previously described an increased intensity of the salt-related deformation toward the north-east, beyond the Thenia fault that separates the Khair al Din bank thrust front from the Kabylia block (Figures 3 and 4a). Toward the south-west, most salt structures are inactive at present, buried under a thick sub-horizontal Plio-Quaternary succession, widely spaced between minibasins. Only a few active diapirs penetrate above the early PQ1 unit at the front of the propagating thick-skinned thrust front (the Khair Al Din bank; Figure 3a,b). The across-strike width of the Algerian foredeep is less than 50 km. Toward the north-east, where the across-strike width increases up to 90 km, the salt structures become more complex and more closely spaced (Figure 3c). Diapirism is still active, recorded by recent growth strata within the PQ3 sequence. Wide salt sheets and salt canopies are observed on top of the UU (Figures 3c and 9). Several factors could control this lateral variability in the intensity of the deformation. We consider the following: (i) an eastward increase in the rate of horizontal tectonic loading, due to segmentation of the margin across the strike-slip Thenia fault; (ii) the variability in salt distribution and precursor structures prior shortening; (iii) a differential thermal loading.

The Algerian margin is described as a transform-type (STEP) segmented margin, that displays contrasting structural domains of contraction and extension, with an important strike slip component (Domzig et al., 2006; Govers & Wortel, 2005; Hamai et al., 2018; Leprêtre, 2012; Medaouri et al., 2014). To the north-east, the convergence rate across the Algerian margin decreases from 3–4 to 1.5 mm/yr (Bougrine et al., 2019; Strzerzynski et al., 2010). However, even though the convergence rate is higher on the south-western segment of the margin, the displacement is mostly accommodated onshore within the Tell Atlas, while shortening along offshore reverse faults is minimal (Arab et al., 2016; Déverchère et al., 2005; Domzig et al., 2006; Leffondré et al., 2021; Yelles et al., 2009). The thick-skinned thrust faults bordering the Khair al Din bank (Figure 4a) may accommodate most of the shortening and focus compressional deformation internally at the margin toe (Figures 1 and 3a,b). Consequently, the displacement loading applied offshore to the salt and overburden may be lower and the deformation milder in the south-west. By contrast, even though the overall

convergence rate is lower to the east of the Thenia fault, it concerns a much broader area and includes a component of strike slip (Domzig et al., 2006; Leffondré et al., 2021; Yelles et al., 2009). Regional shortening is more widely distributed in the outer domain, resulting in a stronger tectonic loading accommodated by the salt and its overburden (Figure 3c).

Alternatively, this along-strike variations in salt deformation could be due to a different salt distribution prior to shortening. It is possible that precursor salt structures were more closely spaced to the east, where a wider basin width allowed the accumulation of a larger salt volume. This is still visible at present, where diapirs are more closely spaced to the east than to the west (Figure 3). The presence of precursor salt structures strongly influence the style of shortening in salt provinces (Duffy et al., 2018; Hudec & Jackson, 2007; Letouzey et al., 1995). To the west, where few, small scale precursor anticlines and diapirs are present, the shortening was accommodated through high amplitude and widely spaced buckling of the overburden. To the east, strain was localized on precursor structures, where salt is thicker, resulting in highly squeezed diapirs and extrusion of salt sheets.

Lastly, thermal loading could potentially influence the variability in style of deformation along the margin. Offshore heat flow measurements showed a westwards increasing trend, from ca. 60 to >150 $mW\,m^{-2}$ (Jiménez-Munt et al., 2003; Poort et al., 2020). This could also have an influence on salt deformation through differential thermal loading, as recently argued by Bellucci, Aslanian, et al. (2021). However, the higher heat flow to the west should induce a higher buoyancy and greater mobility of the salt (Jackson & Hudec, 2017). Therefore, it cannot explain the lower intensity of deformation to the west.

5.5 | The influence of the Emile-Baudot escarpment and the ocean-continent transition

The Balearic slope is divided in two by a WSW-ENE trending topographic high that may have influenced the salt deformation along the Balearic margin. We distinguish the "perched" basin along the EBE, where salt is thin or absent, from an overall basinward dipping ramp, with small amplitude salt structures (Figure 6a,d). Camerlenghi et al. (2009) suggest that this ridge is formed by volcanic rocks intruded along re-activated Miocene normal faults. It would grow by local transtension/transpression along the south-western end of the EBE transform, between the Balearic promontory continental block and the Algerian Basin.

Abrupt termination of the Plio-Quaternary reflections above the crest of the ridge (Figures 6d and 10), and migration of the adjacent PQ depocenters away from the high, suggest that the ridge has been rising since the pre-Messinian, and that it is actively rising at present. The steep seabed pinnacles support the hypothesis that the ridge is partly intruded by volcanic material, as do the steepness of the reflections dipping outward from the crest of the ridge (Figure 10). The interpreted Messinian units are onlapping and pinching out along this ridge, suggesting it was already forming a topographic high at the onset of the MSC (Figure 10).

There is evidence of thin-skinned extension along the Balearic slope expressed by salt-detached normal faults and rollovers of small amplitude (their vertical throw is <15 m, with very small amplitude rotation of the reflector along the fault), suggesting a minor contribution of salt-detached gliding toward the basin (Figures 6 and 7a). Previous studies suggested that these faults could be linked to dewatering of gypsum into anhydrite (Dal Cin et al., 2016; Wardell et al., 2014), but recent overpressure models favoured hydrofracturing induced by over pressured fluids escapes (Dale et al., 2021). We suggest that the faulting is mostly related to extension induced by gravitational instability on a gentle slope. The constant thickness of the UU and PQ1 units suggests that the onset of gliding was approximately coeval with the TOP PQ1 horizon. Because the salt is relatively thin along the Balearic slope, it is possible that frictional boundary forces prevented gliding until the base-salt was sufficiently steepened. This steepening of the Balearic slope can be explained either by subsidence in the deep basin (Dal Cin et al., 2016) or by reactivation of pre-existing basement faults (Camerlenghi et al., 2009) during the regional shortening. This instability could also be related to the presence of MTDs within PQ2 on the Balearic slope (Figure 6d), causing a destabilization event between TOP PQ1 and TOP PQ2.

The deposition of these MTDs and the onset of minor gravity gliding coincide with the general peak of salt tectonic activity previously described across the central Algerian deep basin (around TOP PQ1). We propose that the driving tectonic force that caused the contractional salt deformation within the Balearic ramp (the Top PQ1 shortening event) could have also re-activated the pre-existing Balearic faults. The reactivation of these faults could have steepened the base-salt and caused gravitational instability, triggering minor gravity gliding and mass transport processes. Local small depressions of the seabed suggest that extensional salt tectonics is still active today along the Balearic slope (SP1 in Figure 7).

As suggested by Camerlenghi et al. (2009), the ENE–WSW direction of the salt walls (parallel to the EBE) leads us to think that the salt tectonics is locally influenced by the

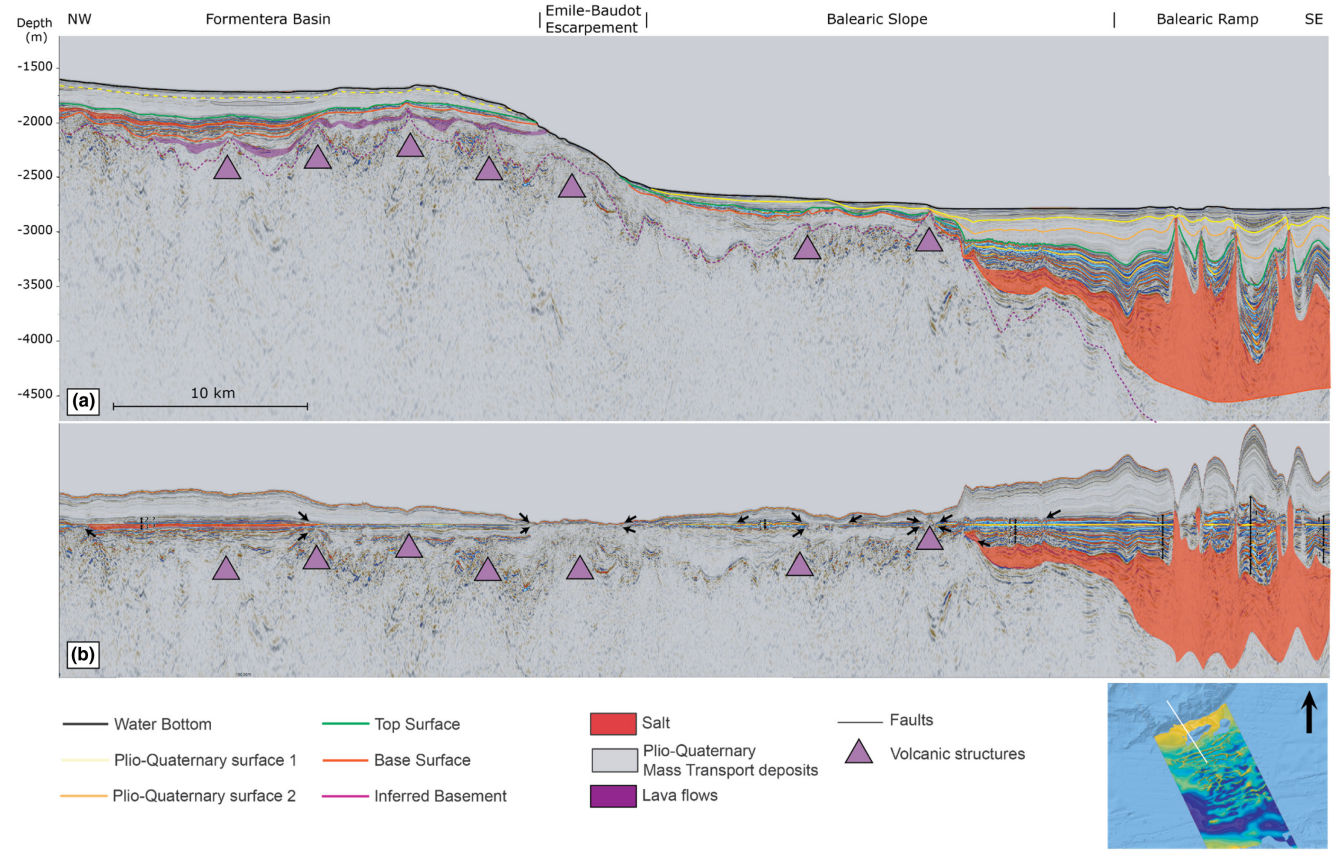

FIGURE 10 (a) Interpreted seismic profile SF07 showing the thinning and the pinching-out of the Messinian units along the basement highs and (b) flattened seismic profile along the strongest regional UU reflector. Location map represents the top salt depth from Figure 4b. Vertical exaggeration ×6

synthetic strike slip fault that borders the ridge (Figure 4b,c). However, we do not interpret this fault to represent the ocean–continent transition (OCT), as previously suggested, because the interpreted base-salt is dipping gently landward and exhibits a base-salt step down from 4500 to 5500 m at the transition zone (Figures 4c and 6). We believe that if there is oceanic crust for this part of the Algerian Basin, it is restricted to the Algerian foredeep domain, where the maximum thickness of Plio-Quaternary sediments is recorded (Figures 3 and 5c). In that scenario, the Balearic ramp could constitute a thinned and stretched continental crust, or a transitional crustal domain. Our results suggest that there are two trends of lineaments in the pre-salt topography (Figure 4c): (i) the ENE-WSW trend parallel to the synthetic EBE strike–slip direction, and (iia) the NW-SE trend parallel to the antithetic EBE strike–slip direction or (iib) the synthetic DJFZ direction and the Thenia fault (Acosta et al., 2013; Boudiaf, 1996). The imaging of the pre-salt and the sparsity of the data do not allow us to accurately identify the tectonic regime, but it is suspected to yield a strange strike-slip component, linked to the important strike-slip escarpment observed at the margins (the EBE, the DJFZ, the NAT). Further geophysical investigations and sampling of the crust could help understanding the nature of the basement here.

5.6 | Messinian to current geological model of the central Algerian Basin

Based on the previous discussions, we suggest a new tectono-sedimentary model for the study area, in the central Algerian Basin (Figure 11):

1. Salt movement begins shortly after deposition of the salt (MU), forming a series of gravity-driven passive salt diapirs throughout the basin (Figure 11). Syn-kinematic deposition of the UU causes differential sedimentary loading of the salt, driving salt spreading and passive diapirism within the central basin. In the Algerian foredeep, the deformation is also driven by the regional shortening at the front of the ongoing inversion of the North African margin, creating small magnitude folds and steepening the base salt-relief.
2. During the deposition of PQ1 the regional shortening starts to increase and to affect the deformation. At

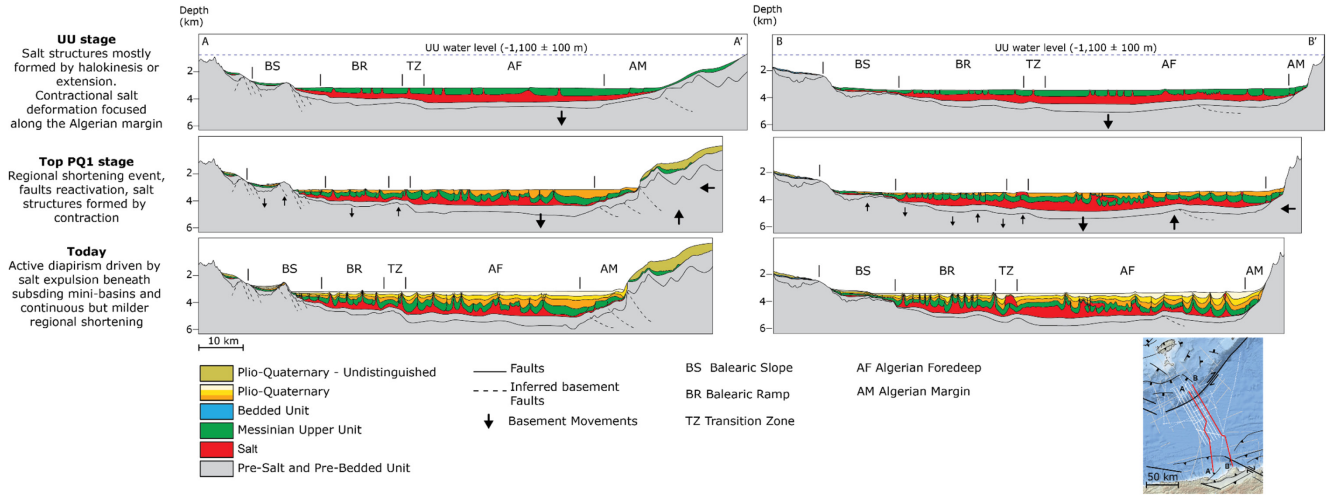

FIGURE 11 Schematic evolution of the basin showing the salt deformation from Messinian to current times along two NW-SE profiles across the central Algerian basin. The water level during the UU deposition is based on estimations from Heida et al. (2021) and Strzerzynski et al. (2021)

early PQ1, diapirs continue to rise mostly passively on the Balearic ramp, but in the Algerian foredeep and in the Transition zone, shortening causes buckling of the overburden and squeezes precursor structures, with local expulsion and inflation of salt sheets at the base of the PQ1. The high aggradation rate of the PQ1 slowly drapes and buries the diapirs. At late PQ1, the shortening starts to affect the Balearic ramp, squeezing the precursor passive diapirs, arching the UU to PQ1 roof above active diapirs and salt-cored anticlines, and rotating the mini basins. Along the EBE, the TOP PQ1 shortening triggers the reactivation of pre-existing rifting faults in the basement, causing the rejuvenation of pre-existing topographic highs, steepening of the base-salt relief and destabilization of the sediments with the deposition of MTDs. The overall deformation creates topographic highs and lows where sediments preferentially accumulate, amplifying the formation of minibasins between salt structures.

3. From TOP PQ1 the deformation seems to be focused predominantly along the Balearic ramp, with actively rising diapirs draped by PQ2 and PQ3. In the Algerian foredeep, the thick roof inhibits the rise of pre-existing salt structures. Deformation is interpreted to be mostly driven by sediment loading, with salt expulsion beneath subsiding minibasins. Locally, in the Algerian foredeep and along the EBE, some actively rising diapirs are uplifting their roof and the seabed, probably driven by ongoing, but milder, regional lateral shortening. Along the EBE, thick-skinned deformation causes minor basinward gliding along a steepened base-salt (post- PQ1 shortening event), inducing an extensional faulting of the UU to current overburden.

6 | CONCLUSION

We used reprocessed 2D seismic reflection data to examine the salt structures in the deep central Algerian Basin, a field analogue of early contractional salt deformation in an incipient orogenic Fold-and-thrust belts. Different structural domains have been recognized based on the thickness of the overburden, the thickness of the salt, and the types of salt structures. We have shown that the central Algerian Basin recorded contractional episodes, with salt-cored anticlines, squeezed diapirs and allochthonous salt sheets. We identified an early Messinian to Zanclean contractional deformation, synchronous with the deposition of the UU, that is more pronounced along the Algerian margin. It is followed by a later Plio-Quaternary deformation, around the TOP PQ1 regional seismic horizon. This later shortening is more pronounced on the Balearic slope because high aggradation rates inhibit further diapirism in the Algerian foredeep. This event could be related to the second phase of inversion of the Atlas system, at Pliocene to lower Quaternary. In the Algerian foredeep, the structural style of salt structures also varies from SW to NE, with an increase in salt deformation toward the NE marked by wide allochthonous salt sheets. We argue that this is controlled by the pre-shortening salt distribution and/or by an increasing tectonic contractional loading from SW to NE. In the south-western part the thick-skinned North African thrust fronts may accommodate most of shortening at the toe of the margin to the SW, while in the north-eastern part of the central Algerian basin, the oblique convergence is more pronounced offshore. We show that the Balearic ramp is mainly landward dipping until a transition zone that is marked by a 500 m base-salt step. We suggest that this transition could be the ocean-continent transition,

with a wide transitional crust along the ramp. Finally, we show that locally along the Balearic slope, the system is currently extensional, driven by the seaward translation of salt and overburden along a steepening base-salt. A continuously rising basement high, parallel to the synthetic Emile-Baudot strike-slip direction, steepened the base salt along which salt could glide more readily, leading to locally extensional salt tectonics that is still active today.

ACKNOWLEDGEMENT

Part of the seismic data used in this project has been processed using the REVEAL© processing software generously provided to the University of Trieste by Shearwater Geoservices. The data were interpreted using the Petrel© software generously provided to the University of Trieste by Schlumberger. The SALTFLU seismic profiles were acquired within EUROFLEETS, call for ship-time 'Ocean' 2010, project 'Salt deformation and sub-salt fluid circulation in the Algero-Balearic abyssal plain—SALTFLU'. EMODnet Bathymetry Consortium (2018): EMODnet Digital Bathymetry (DTM). https://doi.org/10.12770/18ff0d48-b203-4a65-94a9-5fd8b0ec35f6. Open Access Funding provided by Universita degli Studi di Trieste within the CRUI-CARE Agreement.

CONFLICT OF INTEREST

The authors declare that they have no known competing financial interests or personal relationships that could have appeared to influence the work reported in this paper.

PEER REVIEW

The peer review history for this article is available at https://publons.com/publon/10.1111/bre.12673.

DATA AVAILABILITY STATEMENT

The data that support the findings of this study are openly available in Seismic data Network Access Point at https://snap.ogs.trieste.it/.

ORCID

Simon Blondel https://orcid.org/0000-0001-8177-6676
Massimo Bellucci https://orcid.org/0000-0001-6753-5649
Sian Evans https://orcid.org/0000-0003-1083-0019
Angelo Camerlenghi https://orcid.org/0000-0002-8128-9533

REFERENCES

Acosta, J., Ancochea Soto, E., Canals, M., Huertas Coronel, M. J., & Uchupi, E. (2004). Early Pleistocene volcanism in the Emile Baudot Seamount, Balearic Promontory (western Mediterranean Sea). *Marine Geology*, *207*, 247–257.

Acosta, J., Fontán, A., Muñoz, A., Muñoz-Martín, A., Rivera, J., & Uchupi, E. (2013). The morpho-tectonic setting of the Southeast margin of Iberia and the adjacent oceanic Algero-Balearic Basin. *Marine and Petroleum Geology*, *45*, 17–41. https://doi.org/10.1016/j.marpetgeo.2013.04.005

Acosta, J., Muñoz, A., Herranz, P., Palomo, C., Ballesteros, M., Vaquero, M., & Uchupi, E. (2001). Geodynamics of the Emile Baudot Escarpment and the Balearic Promontory, western Mediterranean. *Marine and Petroleum Geology*, *18*, 349–369. https://doi.org/10.1016/S0264-8172(01)00003-4

Arab, M., Belhai, D., Granjeon, D., Roure, F., Arbeaumont, A., Rabineau, M., Bracene, R., Lassal, A., Sulzer, C., & Deverchere, J. (2016). Coupling stratigraphic and petroleum system modeling tools in complex tectonic domains: Case study in the North Algerian Offshore. *Arabian Journal of Geosciences*, *9*, 289. https://doi.org/10.1007/s12517-015-2296-3

Bellucci, M., Aslanian, D., Moulin, M., Rabineau, M., Leroux, E., Pellen, R., Poort, J., Del Ben, A., Gorini, C., & Camerlenghi, A. (2021). Salt morphologies and crustal segmentation relationship: New insights from the Western Mediterranean Sea. *Earth-Science Reviews*, *222*, 103818. https://doi.org/10.1016/j.earscirev.2021.103818

Bellucci, M., Pellen, R., Leroux, E., Bache, F., Garcia, M., Do Couto, D., Raad, F., Blondel, S., Rabineau, M., Gorini, C., Moulin, M., Maillard, A., Lofi, J., Del Ben, A., Camerlenghi, A., Poort, J., & Aslanian, D. (2021). A comprehensive and updated compilation of the seismic stratigraphy markers in the Western Mediterranean Sea. https://doi.org/10.17882/80128

Billi, A., Faccenna, C., Bellier, O., Minelli, L., Neri, G., Piromallo, C., Presti, D., Scrocca, D., & Serpelloni, E. (2011). Recent tectonic reorganization of the Nubia-Eurasia convergent boundary heading for the closure of the western Mediterranean. *Bulletin de la Société Géologique de France*, *182*, 279–303. https://doi.org/10.2113/gssgfbull.182.4.279

Bonvalot, S., Balmino, G., Briais, A., M, K., Peyrefitte, A., N, V., Biancale, R., Gabalda, G., Moreaux, G., Reinquin, F., Sarrahilh, M., Ccgm, C., 2012. World Gravity Map *1*:50M. https://doi.org/10.14682/2012GRAVISOST

Booth-Rea, G., Ranero, C. R., Martínez-Martínez, J. M., & Grevemeyer, I. (2007). Crustal types and Tertiary tectonic evolution of the Alborán sea, western Mediterranean. *Geochemistry, Geophysics, Geosystems*, *8*(10), Q10005. https://doi.org/10.1029/2007gc001639

Boudiaf, A. (1996). Etude sismotectonique de la région d'Alger et de la Kabylie (Algérie): utilisation des modèles numériques de terrains (MNT) et de la télédétection pour la reconnaissance des structures tectoniques actives: contribution à l'évaluation de l'aléa sismique (PhD Thesis).

Bougrine, A., Yelles-Chaouche, A. K., & Calais, E. (2019). Active deformation in Algeria from continuous GPS measurements. *Geophysical Journal International*, *217*, 572–588. https://doi.org/10.1093/gji/ggz035

Burollet, P. F., Said, A., Trouve, P. (1978). *Slim holes drilled on the Algerian Shelf*. Initial Reports of the Deep Sea Drilling Project, Leg 42B, Istanbul, Turkey, to Istanbul, Turkey, May–June 1975, 42, 1181.

Camerlenghi, A., Accettella, D., Costa, S., Lastras, G., Acosta, J., Canals, M., & Wardell, N. (2009). Morphogenesis of the SW Balearic continental slope and adjacent abyssal plain, Western Mediterranean Sea. *International Journal of Earth Sciences*, *98*, 735–750. https://doi.org/10.1007/s00531-008-0354-8

Camerlenghi, A., Wardell, N., Mocnik, A., Del Ben, A., Geletti, R., & Urgeles, R. (2018). 2.C- Algero-Balearic basin. In J. Lofi (Ed.), *Seismic Atlas of the Messinian Salinity Crisis Markers in the Mediterranean Sea, Vol. 2 - Mem. Soc. géol. fr., n.s., 2018, t. 181, and Commission for the Geological Map of the World*, pp. 14–17.

CIESM. (2008). The Messinian Salinity Crisis from mega-deposits to microbiology—A consensus report, in: CIESM Workshop Monographs. Ciesm Monaco, pp. 1–168.

Comas, M. C., Zahn, R., Klaus, A., Aubourg, C., Belanger, P. E., Bernasconi, S. M., Cornell, W., de Kaenel, E. P., de Larouzière, F. D., Doglioni, C., Doose, H., Fukusawa, H., Hobart, M., Iaccarino, S. M., Ippach, P., Marsaglia, K., Meyers, P., Murat, A., O'Sullivan, G. M., ..., Tribble, J. S., Wilkens, R. H. (1996). Proceedings of the Ocean Drilling Program; initial reports; Mediterranean Sea II, the western Mediterranean; covering Leg 161 of the cruises of the drilling vessel JOIDES Resolution, Naples, Italy to Málaga, Spain, sites 974–979, 3 May–2 July 1995. Texas A & M University, Ocean Drilling Program, College Station, TX.

Dal Cin, M., Del Ben, A., Mocnik, A., Accaino, F., Geletti, R., Wardell, N., Zgur, F., & Camerlenghi, A. (2016). Seismic imaging of Late Miocene (Messinian) evaporites from Western Mediterranean back-arc basins. *Petroleum Geoscience*, *22*, 297–308. https://doi.org/10.1144/petgeo2015-096

Dale, M. S., Marín-Moreno, H., Falcon-Suarez, I. H., Grattoni, C., Bull, J. M., & McNeill, L. C. (2021). The Messinian Salinity Crisis as a trigger for high pore pressure development in the Western Mediterranean. *Basin Research*, *33*, 2202–2228. https://doi.org/10.1111/bre.12554

Davis, D. M., & Engelder, T. (1985). The role of salt in fold-and-thrust belts. *Tectonophysics, Collision Tectonics: Deformation of Continental Lithosphere*, *119*, 67–88. https://doi.org/10.1016/0040-1951(85)90033-2

Davison, I., Anderson, L., & Nuttall, P. (2012). Salt deposition, loading and gravity drainage in the Campos and Santos salt basins. *Geological Society, London, Special Publications*, *363*(1), 159–174. https://doi.org/10.1144/sp363.8

Del Ben, A., Mocnik, A., Camerlenghi, A., Geletti, R., & Zgur, F. (2018). 9-Western Sardinia, in: Seismic Atlas of the Messinian Salinity Crisis Markers in the Mediterranean Sea, Vol. 2 - CCGM - CGMW. Mem. Soc. géol. fr., n.s., 2018, t. 181, and Commission for the Geological Map of the World.

DeMets, C., Iaffaldano, G., & Merkouriev, S. (2015). High-resolution Neogene and Quaternary estimates of Nubia-Eurasia-North America Plate motion. *Geophysical Journal International*, *203*, 416–427. https://doi.org/10.1093/gji/ggv277

Déverchère, J., Yelles, K., Domzig, A., Mercier de Lépinay, B., Bouillin, J.-P., Gaullier, V., Bracène, R., Calais, E., Savoye, B., Kherroubi, A., Le Roy, P., Pauc, H., & Dan, G. (2005). Active thrust faulting offshore Boumerdes, Algeria, and its relations to the 2003 Mw 6.9 earthquake. *Geophysical Research Letters*, *32*(4) Portico. https://doi.org/10.1029/2004gl021646

Domzig, A., Yelles, K., Le Roy, C., Déverchère, J., Bouillin, J.-P., Bracène, R., Mercier de Lépinay, B., Le Roy, P., Calais, E., Kherroubi, A., Gaullier, V., Savoye, B., & Pauc, H. (2006). Searching for the Africa–Eurasia Miocene boundary offshore western Algeria (MARADJA'03 cruise). *Comptes Rendus Geoscience, Quelques développements récents sur la géodynamique du Maghreb*, *338*, 80–91. https://doi.org/10.1016/j.crte.2005.11.009

Dooley, T. P., Jackson, M. P. A., & Hudec, M. R. (2009). Inflation and deflation of deeply buried salt stocks during lateral shortening. *Journal of Structural Geology*, *31*, 582–600. https://doi.org/10.1016/j.jsg.2009.03.013

Driussi, O., Maillard, A., Ochoa, D., Lofi, J., Chanier, F., Gaullier, V., Briais, A., Sage, F., Sierro, F., & Garcia, M. (2015). Messinian Salinity Crisis deposits widespread over the Balearic Promontory: Insights from new high-resolution seismic data. *Marine and Petroleum Geology*, *66*, 41–54. https://doi.org/10.1016/j.marpetgeo.2014.09.008

Duffy, O. B., Dooley, T. P., Hudec, M. R., Jackson, M. P. A., Fernandez, N., Jackson, C. A.-L., & Soto, J. I. (2018). Structural evolution of salt-influenced fold-and-thrust belts: A synthesis and new insights from basins containing isolated salt diapirs. *Journal of Structural Geology*, *114*, 206–221. https://doi.org/10.1016/j.jsg.2018.06.024

Etheve, N., Frizon de Lamotte, D., Mohn, G., Martos, R., Roca, E., & Blanpied, C. (2016). Extensional vs contractional Cenozoic deformation in Ibiza (Balearic Promontory, Spain): Integration in the West Mediterranean back-arc setting. *Tectonophysics*, *682*, 35–55. https://doi.org/10.1016/j.tecto.2016.05.037

Flinch, J. F., & Soto, J. I. (2017). Chapter 19—Allochthonous Triassic and Salt Tectonic Processes in the Betic-Rif Orogenic Arc. In J. I. Soto, J. F. Flinch, & G. Tari (Eds.), *Permo-Triassic Salt Provinces of Europe, North Africa and the Atlantic Margins* (pp. 417–446). Elsevier. https://doi.org/10.1016/B978-0-12-809417-4.00020-3

Frizon de Lamotte, D., Bezar, B. S., Bracène, R., & Mercier, E. (2000). The two main steps of the atlas building and geodynamics of the western Mediterranean. *Tectonics*, *19*, 740–761. https://doi.org/10.1029/2000TC900003

Govers, R., & Wortel, M. J. R. (2005). Lithosphere tearing at STEP faults: Response to edges of subduction zones. *Earth and Planetary Science Letters*, *236*, 505–523. https://doi.org/10.1016/j.epsl.2005.03.022

Graham, R., Jackson, M., Pilcher, R., & Kilsdonk, B. (2012). Allochthonous salt in the sub-Alpine fold–thrust belt of Haute Provence, France. In G. I. Alsop, S. G. Archer, A. J. Hartley, N. T. Grant, & R. Hodgkinson (Eds.), *Salt tectonics, sediments and prospectivity* (pp. 595–615). Geological Society of London. https://doi.org/10.1144/SP363.30

Granado, P., Roca, E., Strauss, P., Pelz, K., & Muñoz, J. A. (2018). Structural styles in fold-and-thrust belts involving early salt structures: The Northern Calcareous Alps (Austria). *Geology*, *47*, 51–54. https://doi.org/10.1130/G45281.1

Gueguen, E., Doglioni, C., & Fernandez, M. (1998). On the post-25 Ma geodynamic evolution of the western Mediterranean. *Tectonophysics*, *298*, 259–269. https://doi.org/10.1016/S0040-1951(98)00189-9

Gvirtzman, Z., Reshef, M., Buch-Leviatan, O., & Ben-Avraham, Z. (2013). Intense salt deformation in the Levant Basin in the middle of the Messinian Salinity Crisis. *Earth and Planetary Science Letters*, *379*, 108–119. https://doi.org/10.1016/j.epsl.2013.07.018

Hamai, L., Petit, C., Le Pourhiet, L., Yelles-Chaouche, A., Déverchère, J., Beslier, M.-O., & Abtout, A. (2018). Towards subduction inception along the inverted North African margin of Algeria? Insights from thermo-mechanical models. *Earth and Planetary Science Letters*, *501*, 13–23. https://doi.org/10.1016/j.epsl.2018.08.028

Haq, B., Gorini, C., Baur, J., Moneron, J., & Rubino, J.-L. (2020). Deep Mediterranean's Messinian evaporite giant: How much salt? *Global and Planetary Change*, *184*, 103052. https://doi.org/10.1016/j.gloplacha.2019.103052

Heida, H., Raad, F., Garcia-Castellanos, D., Jiménez-Munt, I., Maillard, A., & Lofi, J. (2021). Flexural-isostatic

reconstruction of the Western Mediterranean during the Messinian Salinity Crisis: Implications for water level and basin connectivity. *Basin Research*, *34*, 50–80. https://doi.org/10.1111/bre.12610

Hsu, K. J., Montadert, L., Bernoulli, D., Bizon, G., Cita, M. B., Erickson, A. J., Fabricius, F. H., Garrison, R. E., Kidd, R. B., Melieres, F., Mueller, C., & Wright, R. C. (1978). Site 371; South Balearic Basin. Initial Reports of the Deep Sea Drilling Project, Leg 42, Part 1, of the cruises of the Drilling Vessel Glomar Challenger; Malaga, Spain, to Istanbul, Turkey, April-May 1975 42, 29.

Hsü, K. J., Ryan, W. B. F., & Cita, M. B. (1973). Late Miocene desiccation of the Mediterranean. *Nature*, *242*, 240–244. https://doi.org/10.1038/242240a0

Hudec, M. R., & Jackson, M. P. A. (2007). Terra infirma: Understanding salt tectonics. *Earth-Science Reviews*, *82*, 1–28. https://doi.org/10.1016/j.earscirev.2007.01.001

Jackson, C., Jackson, M., & Hudec, M. (2015). Understanding the kinematics of salt-bearing passive margins: A critical test of competing hypotheses for the origin of the Albian gap, Santos Basin, offshore Brazil. *Geological Society of America Bulletin*, *127*, 1730–1751. https://doi.org/10.1130/B31290.1

Jackson, M. P. A., & Hudec, M. R. (2017). *Salt tectonics: Principles and practice*. Cambridge University Press.

Jackson, M. P. A., & Vendeville, B. C. (1994). Regional extension as a geologic trigger for diapirism. *GSA Bulletin*, *106*, 57–73. https://doi.org/10.1130/0016-7606(1994)106<0057:REAAGT>2.3.CO;2

Jiménez-Munt, I., Sabadini, R., Gardi, A., & Bianco, G. (2003). Active deformation in the Mediterranean from Gibraltar to Anatolia inferred from numerical modeling and geodetic and seismological data. *Journal of Geophysical Research: Solid Earth*, *108*(B1), ETG 2-1–ETG 2-24. Portico. https://doi.org/10.1029/2001jb001544

Jolivet, L., Augier, R., Robin, C., Suc, J.-P., & Rouchy, J. M. (2006). Lithospheric-scale geodynamic context of the Messinian salinity crisis. *Sedimentary Geology, The Messinian Salinity Crisis Revisited*, *188–189*, 9–33. https://doi.org/10.1016/j.sedgeo.2006.02.004

Krijgsman, W., Hilgen, F. J., Raffi, I., Sierro, F. J., & Wilson, D. S. (1999). Chronology, causes and progression of the Messinian salinity crisis. *Nature*, *400*, 652–655. https://doi.org/10.1038/23231

Leffondré, P., Déverchère, J., Medaouri, M., Klingelhoefer, F., Graindorge, D., & Arab, M. (2021). Ongoing inversion of a passive margin: Spatial variability of strain markers along the Algerian margin and basin (Mediterranean Sea) and Seismotectonic implications. *Frontiers in Earth Science*, *9*, 365. https://doi.org/10.3389/feart.2021.674584

Leprêtre, A. (2012). *Contraintes par imagerie sismique pénétrante sur l'évolution d'une marge Cénozoïque réactivée en compression (cas de la marge algérienne, secteur de Tipaza), Constraints by penetrating seismic imaging on the evolution of a Cenozoic margin reactivated in compression (Algerian margin, sector of Tipaza)* (PhD thesis). Université de Bretagne occidentale.

Leprêtre, A., Klingelhoefer, F., Graindorge, D., Schnurle, P., Beslier, M. O., Yelles, K., Déverchère, J., & Bracene, R. (2013). Multiphased tectonic evolution of the Central Algerian margin from combined wide-angle and reflection seismic data off Tipaza, Algeria. *Journal of Geophysical Research: Solid Earth*, *118*, 3899–3916. https://doi.org/10.1002/jgrb.50318

Letouzey, J., Colletta, B., Vially, R., & Chermette, J. C. (1995). Evolution of salt-related structures in compressional settings. In M. P. A. Jackson, D. G. Roberts, & S. Snelson (Eds.), *Salt tectonics: A global perspective*. American Association of Petroleum Geologists. https://doi.org/10.1306/M65604C3

Li, C., Yin, H., Wu, Z., Zhou, P., Wang, W., Ren, R., Guan, S., Li, X., Luo, H., & Jia, D. (2021). Effects of salt thickness on the structural deformation of foreland fold-and-thrust belt in the Kuqa depression, Tarim basin: Insights from discrete element models. *Frontiers in Earth Science*, *9*. https://doi.org/10.3389/feart.2021.655173

Lofi, J. (2018). Seismic atlas of the Messinian salinity crisis markers in the Mediterranean sea. Mem. Soc. géol. fr., n.s., 2018, t. 181, and Commission for the Geological Map of the World.

Lundin, E. R. (1992). Thin-skinned extensional tectonics on a salt detachment, northern Kwanza Basin, Angola. *Marine and Petroleum Geology*, *9*, 405–411. https://doi.org/10.1016/0264-8172(92)90051-F

Manzi, V., Gennari, R., Hilgen, F., Krijgsman, W., Lugli, S., Roveri, M., & Sierro, F. J. (2013). Age refinement of the Messinian salinity crisis onset in the Mediterranean. *Terra Nova*, *25*, 315–322. https://doi.org/10.1111/ter.12038

Mauffret, A., Frizon de Lamotte, D., Lallemant, S., Gorini, C., & Maillard, A. (2004). E–W opening of the Algerian Basin (Western Mediterranean). *Terra Nova*, *16*, 257–264. https://doi.org/10.1111/j.1365-3121.2004.00559.x

Medaouri, M., Déverchère, J., Graindorge, D., Bracene, R., Badji, R., Ouabadi, A., Yelles-Chaouche, K., & Bendiab, F. (2014). The transition from Alboran to Algerian basins (Western Mediterranean Sea): Chronostratigraphy, deep crustal structure and tectonic evolution at the rear of a narrow slab roll-back system. *Journal of Geodynamics*, *77*, 186–205. https://doi.org/10.1016/j.jog.2014.01.003

Meyer, B., Saltus, R., & Chulliat, A. (2017). *EMAG2v3: Earth Magnetic Anomaly Grid (2-arc-minute resolution). Version 3*. NOAA. https://doi.org/10.7289/V5H70CVX

Mianaekere, V., & Adam, J. (2020). 'Halo-kinematic' sequence stratigraphic analysis adjacent to salt diapirs in the Deepwater contractional province, Liguro-Provençal Basin, Western Mediterranean Sea. *Marine and Petroleum Geology*, *115*, 104258. https://doi.org/10.1016/j.marpetgeo.2020.104258

Mocnik, A., Camerlenghi, A., Del Ben, A., Geletti, R., Wardell, N., & Zgur, F. (2014). The Messinian Salinity Crisis in the West-Mediterranean Basins: Comparison between two rifted margins. In *33rd GNGTS Conference, Bologna*, pp. 156–163.

Najafi, M., & Lajmorak, S. (2020). Contractional salt-tectonic system in the south Dezful embayment, Zagros. *Journal of Structural Geology*, *141*, 104204. https://doi.org/10.1016/j.jsg.2020.104204

Pichel, L. M., Huuse, M., Redfern, J., & Finch, E. (2019). The influence of base-salt relief, rift topography and regional events on salt tectonics offshore Morocco. *Marine and Petroleum Geology*, *103*, 87–113. https://doi.org/10.1016/j.marpetgeo.2019.02.007

Poort, J., Lucazeau, F., Gal, V., Le Cin, M., Dal Leroux, E., Bouzid, A., Rabineau, M., Palomino, D., Battani, A., Akhmanov, G. G., Ferrante, G. M., Gafurova, D. R., Bachir, R., Si Koptev, A., Tremblin, M., Bellucci, M., Pellen, R., Camerlenghi, A., Migeon, S., … Khlystov, O. M. (2020). Heat flow in the Western

Mediterranean: Thermal anomalies on the margins, the seafloor and the transfer zones. *Marine Geology*, *419*, 106064. https://doi.org/10.1016/j.margeo.2019.106064

Quirk, D., Schødt, N., Lassen, B., Ings, S., Hsu, D., Hirsch, K., & von Nicolai, C. (2012). Salt tectonics on passive margins: Examples from Santos, Campos and Kwanza Basins. *Geological Society of London Special Publications*, *363*, 207–244. https://doi.org/10.1144/SP363.10

Raad, F., Lofi, J., Maillard, A., Tzevahirtzian, A., & Caruso, A. (2021). The Messinian Salinity Crisis deposits in the Balearic Promontory: An undeformed analog of the MSC Sicilian basins? *Marine and Petroleum Geology*, *124*, 104777. https://doi.org/10.1016/j.marpetgeo.2020.104777

Recanati, A., Missenard, Y., Leprêtre, R., Gautheron, C., Barbarand, J., Abbassene, F., Abdallah, N., Ouabadi, A., Derder, M. E. M., Boukari, C., Pinna-Jamme, R., & Haurine, F. (2019). A Tortonian onset for the Algerian margin inversion: Evidence from low-temperature thermochronology. *Terra Nova*, *31*, 39–48. https://doi.org/10.1111/ter.12367

Rehault, J.-P., Boillot, G., & Mauffret, A. (1984). The Western Mediterranean Basin geological evolution. *Marine Geology, Geological and Geodynamical Aspects on the Mediterranean*, *55*, 447–477. https://doi.org/10.1016/0025-3227(84)90081-1

Robertson, A. H. F., & Grasso, M. (1995). Overview of the Late Tertiary–Recent tectonic and palaeo-environmental development of the Mediterranean region. *Terra Nova*, *7*, 114–127. https://doi.org/10.1111/j.1365-3121.1995.tb00680.x

Roure, F., Casero, P., & Addoum, B. (2012). Alpine inversion of the North African margin and delamination of its continental lithosphere. *Tectonics*, *31*(3). https://doi.org/10.1029/2011tc002989

Rosenbaum, G., Lister, G., & Duboz, C. (2002). Reconstruction of the tectonic evolution of the Western Mediterranean since the Oligocene. *Journal of the Virtual Explorer*, *8*, 107–130. https://doi.org/10.3809/jvirtex.2002.00053

Rowan, M. G., & Giles, K. A. (2021). Passive versus active salt diapirism. *AAPG Bulletin*, *105*, 53–63. https://doi.org/10.1306/05212020001

Rowan, M. G., Giles, K. A., Hearon, T. E., IV, & Fiduk, J. C. (2016). Megaflaps adjacent to salt diapirs. *AAPG Bulletin*, *100*, 1723–1747. https://doi.org/10.1306/05241616009

Rowan, M. G., Peel, F. J., & Vendeville, B. C. (2004). Gravity-driven fold belts on passive margins. In K. R. McClay (Ed.), *Thrust tectonics and hydrocarbon systems* (pp. 157–182). American Association of Petroleum Geologists. https://doi.org/10.1306/M82813C9

Ryan, W. B. F., Carbotte, S. M., Coplan, J. O., O'Hara, S., Melkonian, A., Arko, R., Weissel, R. A., Ferrini, V., Goodwillie, A., Nitsche, F., Bonczkowski, J., & Zemsky, R. (2009). Global multi-resolution topography synthesis. *Geochemistry, Geophysics, Geosystems*, *10*(3). https://doi.org/10.1029/2008gc002332

Ryan, W. B. F., Hsü, K. J., Cita, M. B., Dumitrica, P., Lort, J. M., Maync, W., Nesteroff, W. D., Pautot, G., Stradner, H., & Wezel, F. C. (1973). Balearic Rise; Site 124. Initial Reports of the Deep Sea Drilling Project, Initial reports of the Deep Sea Drilling Project; covering Leg 13 of the cruises of the Drilling Vessel Glomar Challenger, Lisbon, Portugal to Lisbon, Portugal, August-October 1970 13, 133.

Sans, M. R., & Vergés, J. (1996). Fold development related to contractional salt tectonics: Southeastern Pyrenean thrust front, Spain. *AAPG Memoir*, *65*, 369–378.

Serpelloni, E., Vannucci, G., Pondrelli, S., Argnani, A., Casula, G., Anzidei, M., Baldi, P., & Gasperini, P. (2007). Kinematics of the Western Africa-Eurasia plate boundary from focal mechanisms and GPS data. *Geophysical Journal International*, *25*, 1180–1200. https://doi.org/10.1111/j.1365-246X.2007.03367.x

Soto, J. I., Déverchère, J., Medaouri, M., & Leffondré, P. (2019). *The Messinian Salt Layer Squeezed by Active Plate Convergence in the Western Mediterranean Margins*. Presented at the 2019 AAPG Annual Convention and Exhibition.

Stich, D., Serpelloni, E., de Lis Mancilla, F., & Morales, J. (2006). Kinematics of the Iberia–Maghreb plate contact from seismic moment tensors and GPS observations. *Tectonophysics*, *426*, 295–317. https://doi.org/10.1016/j.tecto.2006.08.004

Strzerzynski, P., Déverchère, J., Cattaneo, A., Domzig, A., Yelles, K., Mercier de Lépinay, B., Babonneau, N., & Boudiaf, A. (2010). Tectonic inheritance and Pliocene-Pleistocene inversion of the Algerian margin around Algiers: Insights from multibeam and seismic reflection data. *Tectonics*, *29*(2). https://doi.org/10.1029/2009tc002547

Strzerzynski, P., Dominguez, S., Boudiaf, A., & Déverchère, J. (2021). Tectonic inversion and geomorphic evolution of the Algerian margin since Messinian times: Insights from new onshore/offshore analog modeling experiments. *Tectonics*, *40*, e2020TC006369. https://doi.org/10.1029/2020TC006369

Trudgill, B. D. (2011). Evolution of salt structures in the northern Paradox Basin: Controls on evaporite deposition, salt wall growth and supra-salt stratigraphic architecture. *Basin Research*, *23*, 208–238. https://doi.org/10.1111/j.1365-2117.2010.00478.x

Uranga, R. M., Ferrer, O., Zamora, G., Muñoz, J. A., & Rowan, M. G. (2022). Salt tectonics of the offshore Tarfaya Basin, Moroccan Atlantic margin. *Marine and Petroleum Geology*, *138*, 105521. https://doi.org/10.1016/j.marpetgeo.2021.105521

Van Hinsbergen, D. J. J., Vissers, R. L. M., & Spakman, W. (2014). Origin and consequences of western Mediterranean subduction, rollback, and slab segmentation. *Tectonics*, *33*, 393–419. https://doi.org/10.1002/2013TC003349

Vergés, J., & Fernàndez, M. (2012). Tethys–Atlantic interaction along the Iberia–Africa plate boundary: The Betic–Rif orogenic system. *Tectonophysics, Orogenic Processes and Structural Heritage in Alpine-Type Mountain Belts*, *579*, 144–172. https://doi.org/10.1016/j.tecto.2012.08.032

Vergés, J., Moragas, M., Martín-Martín, J. D., Saura, E., Casciello, E., Razin, P., Grelaud, C., Malaval, M., Joussiame, R., Messager, G., Sharp, I., & Hunt, D. W. (2017). Chapter 26—Salt Tectonics in the Atlas Mountains of Morocco. In J. I. Soto, J. F. Flinch, & G. Tari (Eds.), *Permo-Triassic Salt Provinces of Europe, North Africa and the Atlantic Margins* (pp. 563–579). Elsevier. https://doi.org/10.1016/B978-0-12-809417-4.00027-6

Verges, J., & Sabat, F. (1999). Constraints on the Neogene Mediterranean kinematic evolution along a 1000 km transect from Iberia to Africa. *Geological Society of London Special Publications*, *156*, 63–80. https://doi.org/10.1144/GSL.SP.1999.156.01.05

Wardell, N., Camerlenghi, A., Urgeles, R., Geletti, R., Tinivella, U., Giustiniani, M., & Accettella, D. (2014). *Seismic evidence for Messinian salt deformation and fluid circulation on the South Balearic margin (Western Mediterranean)*. Presented at the EGU General Assembly Conference Abstracts, p. 11078.

Weijermars, R., Jackson, M. P. A., & Vendeville, B. (1993). Rheological and tectonic modeling of salt provinces. *Tectonophysics*, *217*, 143–174. https://doi.org/10.1016/0040-1951(93)90208-2

Yelles, A., Domzig, A., Déverchère, J., Bracène, R., Mercier de Lépinay, B., Strzerzynski, P., Bertrand, G., Boudiaf, A., Winter, T., Kherroubi, A., Le Roy, P., & Djellit, H. (2009). Plio-Quaternary reactivation of the Neogene margin off NW Algiers, Algeria: The Khayr al Din bank. *Tectonophysics*, *475*, 98–116. https://doi.org/10.1016/j.tecto.2008.11.030

How to cite this article: Blondel, S., Bellucci, M., Evans, S., Del Ben, A. & Camerlenghi, A. (2022). Contractional salt deformation in a recently inverted basin: Miocene to current salt deformation within the central Algerian basin. *Basin Research*, *34*, 1632–1654. https://doi.org/10.1111/bre.12673